DOCUMENT DELIVERY ARTICLE

USC Libraries
Document Delivery
3434 S. Grand Ave. Ste. 208
Los Angeles, CA 90089-2811
(213) 740-4020
(213) 749-1045 (fax)
IDD@usc.edu

Journal Title: Chemical Reactions in Clusters

Article Author: C. Wittig and A.H. Zewail

Article Title: Dynamics of ground state bimolecular reactions

Volume:

Issue:

Month/Year: 1996

Pages: 64-EOA

TN #: 248926

Call #: QD461.C4225 1996

Location: Science And Engineering BOOKSTACKS

NOTE:

PATRON INFORMATION:

Valerie Childress
vchild@usc.edu

STATUS: Staff
DEPT: Chemistry

CSL USE ONLY

☐ UPDATED IN ILLIAD ☐ SENT

Transaction Date: 5/28/2009 06:11:51 PM

3
Dynamics of Ground State Bimolecular Reactions

CURT WITTIG AND AHMED H. ZEWAIL

3.1. INTRODUCTION

During the past decade, the study of photoinitiated reactive and inelastic processes within weakly bound gaseous complexes has evolved into an active area of research in the field of chemical physics. Such specialized microscopic environments offer a number of unique opportunities which enable scientists to examine regiospecific interactions at a level of detail and precision that invites rigorous comparisons between experiment and theory. Specifically, many issues that lie at the heart of physical chemistry, such as reaction probabilities, chemical branching ratios, rates and dynamics of elementary chemical processes, curve crossings, caging, recombination, vibrational redistribution and predissociation, etc., can be studied at the state-to-state level and in real time.

Inevitably, understanding the photophysics and photochemistry of weakly bound complexes lends insight into corresponding processes in less rarefied surroundings, for example, molecules physisorbed on crystalline insulator and metal surfaces, molecules residing on the surfaces of various ices, and molecules weakly solvated in liquids. However, such ties to the real world are not the main driving force behind studies of photoinitiated reactions in complexed gaseous media. Rather, it is the lure of going a step beyond the more common molecular environments. Theoretical modeling, which in many areas purports to challenge experiment, must rise to the occasion here if it is to offer predictive capability for even the simplest of such microcosms. Subtleties abound.

Roughly speaking, two disparate regimes can be identified which are accessible experimentally and which correspond to qualitatively different kinds of chemical transformations. These are distinguished by their reactants: electronically excited versus ground state. For example, it is possible to study the chemical selectivity that derives from the alignment and orientation of excited electronic orbitals, albeit at restricted sets of nuclear coordinates. This is achieved by electronically exciting a complexed moiety, such as a metal atom, which then undergoes chemical transformations that depend on the geometric properties of the electronic orbitals such as their alignments and orientations relative to the other moiety (or moieties)

in the complex. This approach was pioneered by Soep and coworkers (Boivineau et al. 1986a,b; Breckenridge 1989; Breckenridge et al. 1985, 1986 1987; Duval et al. 1985, 1986, 1991; Jouvet et al. 1987, 1989; Jouvet and Soep 1983, 1984, 1985; Loison et al. 1994; Soep 1994), who examined several important prototypical systems in detail by using complementary experimental methods: measurements of excited state spectral properties, product state distributions, and, more recently, time domain studies (Soep 1994).

Alternatively, a number of efforts have focused on systems that involve ground electronic state reactants, or, more precisely, systems in which the photoexcited moiety is known to evolve to ground electronic state fragments in the absence of complexation. For example, HX photodissociation has been used to prepare both hydrogen and halogen atom reactants on time scales which are short, relative to those of subsequent dynamical processes. In many of these cases, it has been possible to infer properties of the corresponding gas phase reactions. This review deals exclusively with this latter class of photoexcited reactions in neutral complexes, namely, those which parallel reactions that occur via the ground potential energy surface (PES), which we take to be the adiabatic one. Also, *binary* complexes will be stressed, though higher-than-binary complexes inevitably enter the picture. In many cases, the geometric properties of the complexes under consideration, such as equilibrium geometries and zero point excursions, are known from spectroscopic studies or can be obtained from theory with good reliability.

To focus the review, it is necessary to pass over some topics which are timely, relevant, and could be included were it not for space limitations. One of these is the area of electron photodetachment as applied to the study of the Franck–Condon region of the neutral PES accessed from the corresponding anion. This approach has been shown to provide information about the transition state region of several bimolecular reactions. This work was pioneered by Neumark and coworkers and an excellent review is already available (Manolopoulos et al. 1993; Neumark 1992). Another noteworthy area is state-to-state studies of vibrational predissociation in weakly bound complexes. Miller and coworkers have made impressive advances in which fully state and angle-resolved product distributions have been obtained (Bemish et al. 1994; Block et al. 1992; Bohac et al. 1986, 1992a,b; Bohac and Miller 1993a,b; Dayton et al. 1989), and these results have been used to bring theory and experiment into accord. The present review is limited to cases in which ultraviolet photodissociation of a complexed moiety initiates reaction.

In writing this review, it is our intention to provide an assessment of where the field stands, as well as where we see it going on the fronts most familiar to the authors. The document is not a compendium, and, as stated previously, some work had to be omitted because of the demand for brevity. Like most areas of science, progress has not been distributed homogeneously in time, nor will it be in the future. Following several early "demonstration of principle" achievements, results have flowed at a steady but modest pace. However, we believe that this is about to change, since a number of milestones have been passed in the last few years. Consequently, we envision an explosion of results that will propel this field to the same level of sophistication that presently exists for studies of stable molecules and radicals.

3.2. PHOTOINITIATED REACTIONS IN CO_2–HX COMPLEXES

3.2.1. Counterparts under Gas Phase, Single-Collision Conditions

The gas phase reaction considered to be a close counterpart to the photoinitiated reaction that occurs in CO_2–HX complexes is:

$$H + CO_2 \rightarrow HOCO^{\dagger} \rightarrow OH + CO \qquad \Delta H = 8960\ cm^{-1}, \qquad (1)$$

where the vibrationally excited $HOCO^{\dagger}$ intermediate decomposes via a unimolecular mechanism (Smith 1980). Note that reaction (1) is written for the *endoergic direction*, i.e., paralleling the reaction that is photoinitiated within weakly bound complexes. On the other hand, the *exoergic* direction is of considerable technical importance, since it is responsible for the oxidation of CO during the combustion of hydrocarbon fuels (Baulch et al. 1984; Davis et al. 1974; Gardiner 1977; Jonah et al. 1984; Mozurkewich et al. 1984a,b; Ravishankara and Thompson 1983; Warnatz 1984). This technical significance accounts in part for the large number of detailed experimental and theoretical studies that have been carried out during the last few decades with this prototypical elementary reaction.

Smith and coworkers have contributed greatly to our understanding of this system through a number of experimental and theoretical contributions, most notably comparing the results of detailed measurements of k_{-1}, that is, the rate constant for the reverse of reaction (1), to predictions made by using them oretical models based on transition state theories (Brunning et al. 1988; Smith 1977, 1980; Smith and Zellner 1973; Zellner and Steinert 1976). This work commenced in the early 1970s and stands as a landmark contribution. They were able to identify details of the potential energy surface through analyses of the various measurements of $k_{-1}(T)$, which span the temperature range $80 \leq T \leq 2000$ K (Frost et al. 1991a, 1993). Specifically, it was shown that the markedly non-Arrhenius temperature dependence shown in Figure 3-1 could be reconciled by using RRKM theory with barriers that have comparable energies for the two chemically distinct $HOCO^{\dagger}$ decomposition channels. Also, by measuring rates at temperatures down to 80 K (Frost et al. 1991a, 1993), they were able to demonstrate unambiguously that there is, at most, a minuscule barrier to the process whereby OH and CO combine to form the $HOCO^{\dagger}$ intermediate. Furthermore, they were able to discern qualitative features of the transition state leading to $H + CO_2$ by measuring the CO_2 vibrational distribution and invoking the reasonable assumption of minimal vibrational energy transfer once the reaction has progressed past the transition state (Frost et al. 1991b).

A full six-dimensional PES for the HOCO system has been developed by Schatz and coworkers, particularly L. B. Harding (Kudla et al. 1992; Schatz et al. 1987). This proved to be challenging because of numerous local minima and transition states, and consequently the development of the PES has taken several years. Many points were calculated by using large scale *ab initio* techniques and the surface was adjusted to reconcile a broad array of experimental data such as nascent product excitations, $HOCO^{\dagger}$ decomposition rates, overall bimolecular reaction rates, barrier heights, enthalpy changes, HOCO structural properties, and inelastic scattering data. This PES has been used in several computational studies of the reaction dynamics that employ classical (Kudla and Schatz 1991; Kudla

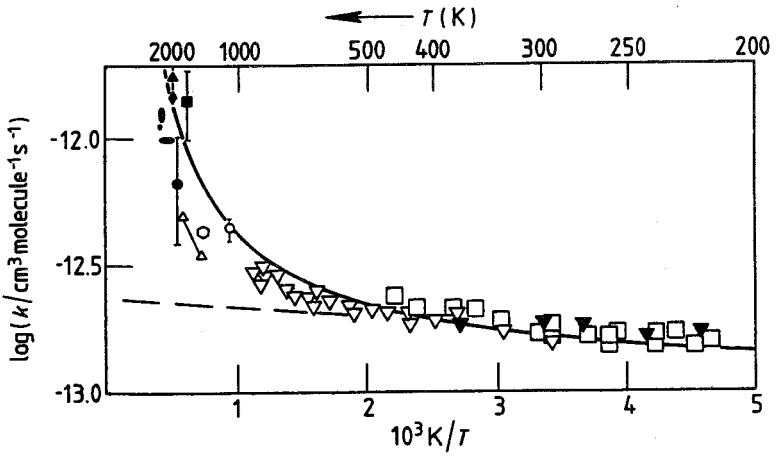

Figure 3-1. Rate constants $k(T)$ for the range $200 \leq T \leq 2000$ K, taken from Smith (1980). Note the decidedly non-Arrhenius behavior. The data below 1000 K are those of Smith and Zellner (1973) (open squares), Davis et al. (1974) (filled triangles), and Zellner and Steinert (1976) (open triangles); points above 1000 K are from the review by Warmatz. The full line shows the result of TST calculations (Smith 1980), while the dashed line is an extrapolation of the Arrhenius expression chosen by Davis et al. (1974) to represent their data in the range 220–373 K. Below 200 K, $k(T)$ remains constant until $\sim$140 K; thereafter it drops to $\sim 1 \times 10^{-13}$ at 80 K (Frost et al. 1991a, 1993).

et al. 1991, 1992; Schatz 1989) and/or quantum mechanical (Clary and Schatz 1993; Hernández and Clary 1994; Schatz and Dyck 1992) methods. Despite its inherent complexities, this surface is one of the best available for a four-atom system. It can reproduce most of the experimental data on reactive and inelastic processes, at least qualitatively. The diagram given in Figure 3-2 shows the low energy reaction path.

The $OH + CO \rightarrow H + CO_2$ reaction has also been examined experimentally by using the crossed molecular beams technique. Casavecchia and coworkers developed an intense molecular beam source of OH radicals which was crossed with a beam of CO in a standard crossed beams arrangement (Alagia et al. 1993). These measurements provided information on product translational and internal excitations for several center-of-mass (c.m.) collision energies. Moreover, it was possible to estimate reaction rates by measuring the angular distributions of products in the c.m. system and comparing these experimental observations with estimates made by using simple models to calculate the rotational periods of the $HOCO^{\dagger}$ intermediate. An example of the scattering anisotropy in the c.m. system is shown in Figure 3-3 (Alagia et al. 1993). Although this is an indirect measure of the lifetime of the intermediate complex, the rates thus obtained are consistent with the measurements discussed below that employ the subpicosecond resolution pump–probe technique, albeit with weakly bound complexes as precursors.

Under 300 K ambient conditions, reactions of photolytically produced fast hydrogen atoms with CO_2 are known to yield OH + CO products via vibrationally excited $HOCO^{\dagger}$ intermediates. Since the initial report by Oldershaw and Porter (1969), many groups have studied reaction (1) by using fast hydrogen atoms and

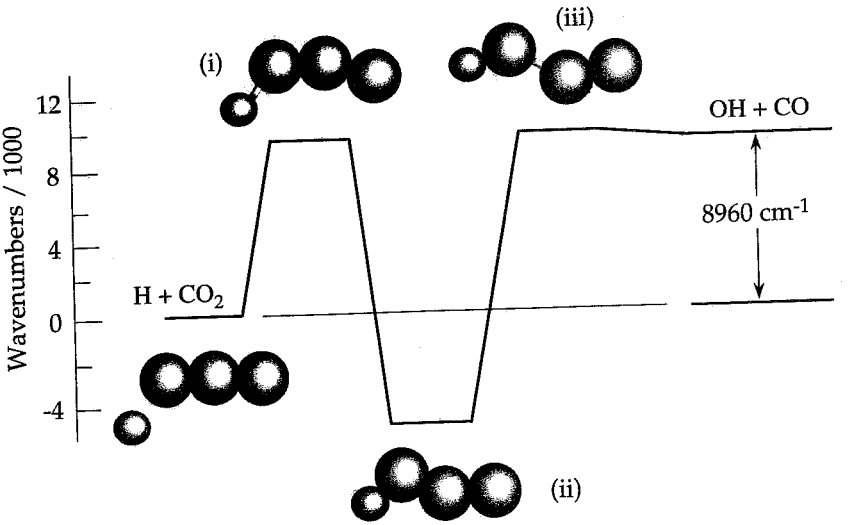

Figure 3-2. Potential energy relative to $H + CO_2$ for selected points on the HOCO PES; from left to right: (i) the transition state for $HOCO \leftrightarrow H + CO_2$, (ii) *trans*-HOCO (*cis*-HOCO and the small *cis–trans* conversion barrier are not shown), and (iii) the transition state for $HOCO \leftrightarrow OH + CO$; from the low temperature rate measurements, this transition state is known to be very loose (Frost et al. 1991a, 1993).

single-collision, arrested-relaxation conditions. Measured quantities include nascent OH and CO internal excitations, product c.m. translational excitations, and reaction cross sections. Moreover, these have been measured as a function of the c.m. collision energy. Wolfrum and coworkers reported absolute cross sections for several collision energies, thereby calibrating the relative cross sections (Jacobs et al. 1989). Additionally, they found little, if any, spatial anisotropy of the OH

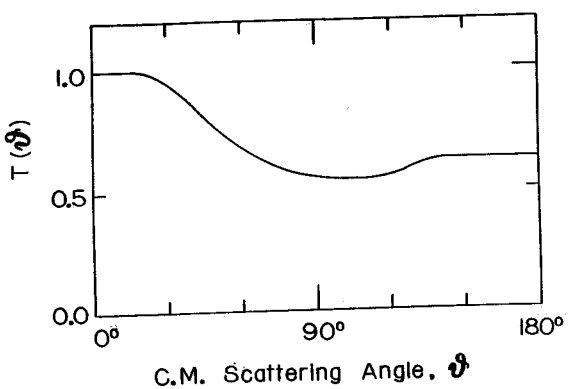

Figure 3-3. Forward/backward asymmetry in the c.m. system for the $H + CO_2$ channel, from the crossed molecular beams experiments of Casavecchia and coworkers (Alagia et al. 1993). This asymmetry can be related to the lifetime of the $HOCO^{\dagger}$ intermediate.

product, in accord with the participation of the $HOCO^{\dagger}$ intermediate (Jacobs et al. 1994). Most of the work involving hot atom $H + CO_2$ reactions has been reviewed recently (Chen et al. 1992; Shin et al. 1991a) and little has accured in the meantime. Thus, it will be summarized briefly in subsection 3.2.3.

With CO_2–HX complexes, the photoinitiated reactions are believed to parallel their uncomplexed counterparts since the halogen does not play a dominant role. Specifically, in a minority of cases Br–C attraction can lead to a short-lived $HO(Br)CO^{\dagger}$ intermediate, as discussed below. Thus, although the photochemistry of CO_2–HX complexes involves five nuclei, it is still meaningful to make comparisons with the gas phase process depicted in reaction (1).

3.2.2. Geometric Properties of CO_2–HX Complexes

For a given precursor complex, it is most desirable to have a secure knowledge of its spectroscopic and geometric properties before embarking on studies of its photochemistry. Unfortunately, such information is not always available. In fact, some of the more attractive systems from the perspective of photoinitiated reactions in complexes have been viewed as relatively uninteresting by high resolution spectroscopists who specialize in determining and understanding structure and bonding of weakly bound complexes. As a group, they have preferred to work with light elements and simpler systems, since these are amenable to a fairly high level of theory.

On the other hand, a natural inclination of experimentalists trying to use photodissociation as a means of preparing reactants is to exploit convenient ultraviolet wavelengths. This prejudices one toward molecules that contain heavy elements. Presently, the most feasible experiments in which hydrogen atoms are required involve photoinitiated reactions in weakly bound complexes that contain molecules like HI and HBr. For example, one of our favorite sources of atomic hydrogen is HI, since direct, one-photon photodissociation occurs via a broad continuum that extends from the vacuum ultraviolet to $\sim$280 nm. Hydrogen bromide runs second, while HCl is barely accessible at 193 nm and HF absorbs only in the vacuum ultraviolet. This order of preference will change in the future as double resonance photodissociation of HX moieties within complexes gains acceptance, but for the time being the ultral violet absorption spectra of the constituents of weakly bound complexes is an important, practical consideration.

The best means of determining the geometric properties of weakly bound complexes is high resolution spectroscopy in combination with theoretical models that treat explicitly the large amplitude motions. However, in some cases structural properties can also be determined with acceptable accuracy by using theory alone. Specifically, semiempirical methods based on the concepts of classical electrostatics are known to give reliable results, as has been shown, for example, by Dykstra (1990) and coworkers. In most cases, these semiempirical approaches are at least as accurate as the brute force application of large scale *ab initio* methods to calculate the weak interaction directly. However, even with these semiempirical approaches there is a reluctance to go to the heavier elements because accurate electronic structure calculations are usually needed to provide properties such as

polarizabilities. Nonetheless, we believe that it is possible to make reasonable estimates of structural properties in systems for which there are no (or limited) experimental data.

The geometric properties of weakly bound CO_2–HF and CO_2–HCl complexes have been established from high resolution spectroscopic studies (Altman et al. 1982; Baiocchi et al. 1981; Lovejoy et al. 1987; Nesbitt 1988; Nesbitt and Lovejoy 1990, 1992; Shea et al. 1983). They are both quasilinear, exhibiting hinge-like, large amplitude zero point excursions for the lowest frequency bending mode. For example, Shea et al. (1983) examined the rotational Zeeman effect in CO_2–HF and CO_2–HCl by using a pulsed Fourier transform microwave spectrometer. Zero field rotational spectra of $O^{13}CO$–HF(HCl) and $^{18}OC^{18}O$–HF(HCl) were recorded, and it was found that the expectation values of the angles between the *a*-axis and the CO_2 and HF axes were $\langle\chi\rangle \sim 12°$ and 24°, respectively. Note that these values are half the *full* angular widths. Thus, it is clear that large amplitude hinge-like motion is present, with a factor of approximately two difference in the $\langle\chi\rangle$ values for CO_2 and HF. Furthermore, since the dominant intermolecular attractive force for these complexes is hydrogen bonding, CO_2–HCl is floppier than CO_2–HF.

On the other hand, CO_2–HBr was found to be different. The bromine faces the carbon with a Br–C–O angle of approximately 90°, in what we refer to as an inertially T-shaped structure (Sharpe et al. 1990; Zeng et al. 1992). Unfortunately, the accuracy of our measurements was insufficient to locate the hydrogen. It is reasonable for it to be localized near the oxygen, even though hydrogen bonding is not the *dominant* interaction.

This qualitative change in going from CO_2–HCl to CO_2–HBr was attributed to the presence of two attractive interactions that compete to determine the equilibrium geometry: hydrogen bonding versus polarization of the halogen electron density by the substantial CO_2 quadrupole moment. The latter interaction dominates in CO_2–HBr, though from electronic structure calculations we concluded that the competition is close (Zeng et al. 1992). Unfortunately, no spectroscopic evidence has ever been reported which supports the existence of a quasilinear CO_2–HBr isomer.

This competition between weak hydrogen bonding and polarization of the bromine depends sensitively on molecular properties. For example, consider the case of SCO–HX complexes, for which both SCO–HF and SCO–HCl have been found to be linear as shown; that is, the HX is hydrogen-bonded to the oxygen (Altman et al. 1982; Baiocchi et al. 1981; Fraser et al. 1989; Legon and Willoughby 1985; Shea et al. 1983). These are analogous to CO_2–HF and CO_2–HCl. However, it has been discovered recently that SCO–HBr is *also* linear as shown (Hu and Sharpe 1994; Walker et al. submitted), in contrast to inertially T-shaped CO_2–HBr. This qualitative structural difference underscores both the subtle competitions that occur in such systems and the need for experimental structural determinations.

For CO_2–HBr, rotation about the *a*-axis, which lies close to a line connecting the carbon and bromine nuclei, is analogous to the rotation of free CO_2. However, it was found that the oxygen atoms do not occupy equivalent sites in the complex; that is, the hydrogen stays near one oxygen for the time scale of the spectroscopic observation. Specifically, if the wavefunction of the complex possesses C_{2v}

symmetry, Bose–Einstein statistics require that all odd K_a values are missing in the lower state, as has been observed with CO_2/rare gas complexes (Randall et al. 1988; Sharpe et al. 1988). This is definitely not the case. Both even and odd K_a states are found in the lower and upper states, indicating that the H atom probability density is not symmetric about the C_{2v} axis on the time scale of the measurement. We interpret this as an indication that the H atom is probably localized near one of the oxygen atoms.

By exploiting the higher resolution available with microwave spectroscopy, it was possible to locate the HBr axis relative to the *a*-axis and it was found that this angle has an average value of approximately 100° (Rice et al. 1995). However, by itself, the measurement is *also* consistent with an average H–Br–C angle of approximately 80°. In principle, if the zero point amplitude is very large, both equilibrium angles could prove to be consistent with the photoinitiated reaction studies. By obtaining slices on the intermolecular potential surface, it was possible to calculate approximate wavefunctions for some of the intermolecular degrees of freedom (Zeng et al. 1992), and this confirmed the large amplitude hydrogen motion.

From the above considerations, it follows that CO_2–HI will most probably be inertially T-shaped, with at least as large a hydrogen zero point amplitude as for the case of CO_2–HBr. There is no fundamental reason why the structure of this complex has not yet been measured. We attempted this once by using high resolution infrared tunable diode laser spectroscopy and confirmed the inertially T-shaped character (Lin et al. n.d). However, before accurate rotational constants could be obtained, the HI ruined the vacuum pump, as it is prone to do. This lessened our appetite for a more precise structural determination.

3.2.3. Frequency Domain Studies

Since photoinitiated reactions in CO_2–HX complexes have been studied more than those in any other weakly bound complex, they will be one of our main points of concentration. The first studies of this system examined the disposal of the available energy into product degrees of freedom, as well as a steric effect; specifically, how the reaction probability changes for end-on versus broadside hydrogen approaches (Shin et al. 1990). This was followed by time domain studies in which the close proximity of the complexed molecules provided a well defined $t = 0$ marker (Scherer et al. 1987, 1990). Although this concept is universal, it is especially appropriate when photodissociation yields atomic hydrogen, with its high characteristic speed. Here, we review the status of frequency domain measurements made between 1985 and the present, before moving to the more recent time domain studies.

As stated above, high resolution spectroscopic studies indicate that a qualitative change occurs in going from the quasilinear complexes containing HF and HCl to inertially T-shaped CO_2–HBr, and it is safe to assume that CO_2–HI is also inertially T-shaped. Because HF forms very directional hydrogen bonds with Lewis bases, complexes such as CO_2–HF are especially attractive. However, there is a serious experimental complication: HF absorption lies deep in the vacuum

ultraviolet, peaking near 125 nm (Lee 1985). Thus, its use in studies of weakly bound complexes will likely be restricted to double resonance photodissociation, as described below. Nonetheless, we predict that it will play a prominent role in future research.

a. *Nascent* $OH(X^2\Pi)$ *excitations*

For the CO_2–HX systems under consideration, every measurement to date of nascent OH excitations obtained under complexed conditions has shown that there is less OH internal energy than for the case of the corresponding gas phase reaction. This is to be expected, on the basis of the naive argument that complexed systems have larger heat capacities than their uncomplexed gas phase counterparts. Consequently, if statistics prevails, OH deriving from complexes will have less internal energy than OH deriving from the gas phase reaction (1) at the same total energy.

On the basis of simple dynamical and kinematic considerations, as well as a minimal entropy analysis of the product state distributions, we concluded that $HOCO^\dagger$ intermediates formed via complexes had less internal energy than those formed via the corresponding gas phase reaction (Wittig et al. 1988a,b). This was easy to rationalize. One obvious factor is the squeezed atom effect (Wittig et al. 1988a). Here, the photoinitiated transfer of the hydrogen atom from the halogen to CO_2 results in recoil between the HOCO and halogen atom products. Specifically, in the process of being transferred from the halogen to CO_2, the light hydrogen pushes against its heavier surroundings, and the resulting increase in X–HOCO recoil comes at the expense of HOCO internal excitation. An analogous effect has been observed in clusters of HBr with Ar, where the recoil energy was observed to be $\sim 10\%$ of the total available energy (Segall et al. 1993). Furthermore, this is consistent with theoretical predictions (Alimi and Gerber 1990; Garcia-Vela et al. 1991, 1992).

Additionally, we speculated that the lowest OH internal excitations (i.e., $v = 0$, low N) might derive preferentially from higher-than-binary complexes and/or a mechanism that involves a five-atom HO(Br)CO intermediate produced by a multicenter process following photoexcitation (Hoffmann et al. 1990).

Because of the entrance channel regiospecificity, the question has often been asked: is it possible that the different OH level distributions relative to the gas phase are simply due to the restricted set of hydrogen approach angles and impact parameters? We think not, because this would require the $HOCO^\dagger$ intermediate to behave quite nonstatistically, and under the present experimental conditions this seems unlikely. This will be discussed further in subsection 3.2.4.

b. *Higher-than-binary complexes*

Over the years, several experiments were carried out to address the issue of higher complexes. Originally, mass spectrometer signals were recorded simultaneously with the OH LIF signals, while the experimental conditions (i.e., signal strengths) were varied (Radhakrishnan et al. 1986). It was found that the CO_2HBr^+ mass spectrometer signal varied linearly with the OH LIF signal. On the other hand,

signals from $(CO_2)_2HBr^+$ and $CO_2(HBr)_2^+$ varied faster than linearly with the OH LIF signal. This was taken as support for the contention that the OH yield derived mainly from binary complexes. However, this experiment did not provide *proof* because of the unclear relationship between the concentration of a given neutral cluster and the mass spectrometer signal that appears at that mass. For example, does CO_2HBr^+ derive from CO_2–HBr or from higher neutral clusters, which are known to crack into smaller units following electron impact ionization? Because of this ambiguity, it is possible that the CO_2HBr^+ signal is not a monitor of CO_2HBr, but is some unknown function of the cluster size distribution. Later, it was shown that the CO_2HBr^+ signal varied linearly with the CO_2–HBr concentration (Shin et al. 1990). This was determined by monitoring CO_2HBr^+ signals while measuring relative CO_2–HBr concentrations using high resolution tunable diode laser spectroscopy with a pulsed slit expansion. Again, this evidence is strongly suggestive but not conclusive. For example, if neutral trimers yield a large CO_2HBr^+ signal and if their concentration tracks that of CO_2–HBr, then their contribution to the OH LIF signal cannot be discerned by measuring the variation of the CO_2HBr^+ signal versus the OH LIF signal. Another caveat is the possibility that the OH yield for one or more of the higher clusters is significantly higher than that for binary clusters. Though there is no evidence suggesting that this is the case, it is best to leave open the possibility.

From the above considerations, we conclude that isolating contributions from clusters of different sizes is a task of serious proportions. A foolproof diagnostic is called for, and this leads inevitably to methods that enable weakly bound complexes to be size selected. Without reliable size selection, every case will be "special" and progress will accrue slowly, since many checks will be required to build a case based on circumstantial evidence.

Ultimately, we would like to *choose* different complexes (dimers, trimers, tetramers, etc.), but given the present state of affairs, isolating contributions from binary complexes will suffice, at least for the time being. Because of its paramount importance, this issue will be discussed further and proposed solutions will be outlined in section 3.4, which is devoted to prospects for future research. Of the two approaches that are most viable, that is, molecular beam deflection (Buck 1994) and laser-based double-resonance methods, the former is superior for larger clusters while the latter is superior for binary complexes, as well as offering state selection. Consequently, we prefer the latter for the near future. Specifically, an infrared laser can be used to excite HX moieties within binary complexes, thereby tagging the complexes via the spectral resolution that enables them to be distinguished from monomers, trimers, etc. These vibrationally excited HX moieties are then photodissociated at wavelengths that leave the untagged complexes unaffected. In this way, weakly bound complexes are both size selected, and, in many cases, state selected. This method is depicted schematically in Figure 3-4. It is our judgment that the double resonance method is well suited to a broad range of systems and will yield qualitative advances. Furthermore, the approach is applicable to ultrafast as well as nanosecond techniques. Such experiments are within reach using technology that is essentially off-the-shelf, and examples will be given of recent experimental results that establish the viability of this approach.

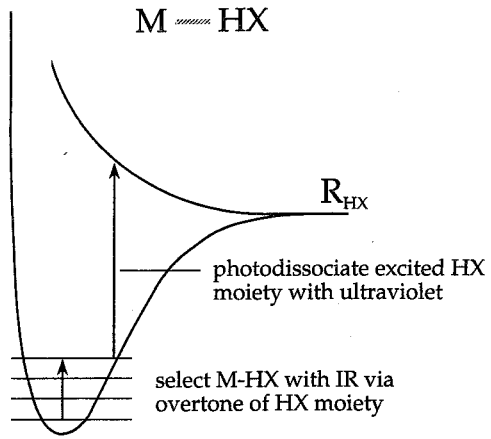

Figure 3-4. Schematic of size and state selection of weakly bound complexes. Weak M–HX intermolecular coupling and the corresponding long predissociation lifetimes enable ro-vibrational levels of the complex to be isolated. Ultraviolet photons at sufficiently long wavelengths act on the excited (but not the unexcited) HX moieties.

3.2.4. Time Domain Studies

In 1987, the picosecond-resolution pump–probe technique was applied to the CO_2-HI system, in which reaction is photoinitiated by ultraviolet photodissociation of the HI moiety (Scherer et al. 1987). This was the first case in which the $t = 0$ clocking method, which had been developed earlier for the study of photofragmentation dynamics (Zewail 1988, 1993), was applied to the study of a *bimolecular* reaction, albeit in the unique environment of a complex. A schematic drawing of the concept is given in Figure 3-5. This experiment demonstrated unambiguously that reaction was not direct, that is, it occurred via an intermediate having lifetimes in the picosecond regime. Furthermore, these lifetimes depend on the energy of the photon used to initiate the reaction. The pump and probe pulses were both of several picoseconds duration, and the probe was of sufficiently narrow linewidth that individual OH rotational levels could be resolved. Specifically, data were collected for $N = 1$ and 6. Despite the low photon count rates (typically less than one per laser firing) and the difficulty of the measurements, it was demonstrated

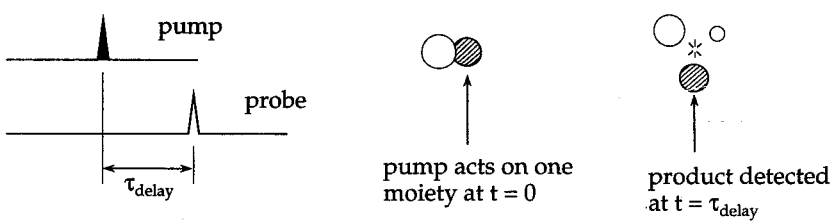

Figure 3-5. Schematic of ultrafast pump–probe method applied to photoinitiated reactions in binary complexes.

that such experiments were indeed possible. Consequently, this result spawned further efforts along similar lines.

Subsequent experiments by Ionov et al. (1992, 1993b) were carried out with better time resolution, enabling OH buildup to be determined with subpicosecond accuracy. These rates were in accord with predictions made by using RRKM theory, where it was assumed that the nearby halogen atom plays no role other than to lower the $HOCO^{\dagger}$ energy by a small amount as per the squeezed atom effect (Wittig et al. 1988a). The parameters used in the RRKM calculations were those obtained by Smith and coworkers from extensive modeling of $k_{-1}(T)$ for the overall $OH + CO \rightarrow H + CO_2$ reaction (Brunning et al. 1988; Smith 1977; Smith and Zellner 1973; Zellner and Steinert 1976). Because of the uncertainty of the $HOCO^{\dagger}$ energy, as well as the likelihood of a distribution of $HOCO^{\dagger}$ energies for a single photolysis wavelength, it was not possible to make an exact comparison between experiment and theory. However, despite the latitude in assigning $E^{\dagger}$ values, agreement was claimed. At the very least, there was no serious *disagreement.*

The time resolved OH buildup measurements all confirmed a unimolecular decomposition mechanism for the photoinitiated reaction in weakly bound CO_2–HI complexes. Though the Ionov et al. (1992, 1993b) rates are larger than those reported by Scherer et al. (1990) (see Figure 3-6), the experiments differ in important respects. For example, in the Ionov et al. experiments, a broadband probe monitors essentially all of the OH rotational levels simultaneously. Therefore, these experiments are sensitive to the average behavior of all processes that yield OH. On the other hand, the Scherer et al. experiments were carried out with OH rotational state resolution, which enabled them to show that the buildup rates for the $N = 1$ rotational level were slower than those for $N = 6$ by as much as 70%. This is noteworthy because unimolecular rate theories predict that all products are produced with the same rate for a microcanonical system undergoing unimolecular decomposition. Thus, one might ask whether or not: (1) the system is behaving nonstatistically, (2) $HOCO^{\dagger}$ intermediates are produced having significantly different $E^{\dagger}$ values, that is, via different mechanisms, and (3) other sources of OH are involved, for example, $HOBr^{\dagger}$. Here, we discuss these possibilities.

It has been known for many years that in low dimensional systems undergoing unimolecular decomposition, reaction rates fluctuate about a mean value which is generally taken to be the statistical one, such as the RRKM rate (Green et al. 1991, 1992; Hernandez and Miller 1993; Manthe and Miller 1993; Polik et al. 1988, 1990a,b). Likewise, product state distributions display irregularities that can be attributed to both the interferences that occur between the different decay paths (i.e., through the different transition state levels) as well as the rapid changes in the product state distributions that are manifestations of so-called chaotic behavior of the parent in the small molecule limit. For example, in the case of NO_2, it has been shown that product state distributions appear to be statistical when sufficient averaging is done over the decaying parent resonances, while with good parent energy resolution, the product level distributions fluctuate as per the mappings and interferences of transition state levels projected onto the product degrees of freedom (Hunter et al. 1993; Peskin et al. 1994; Reid et al. 1993a,b; Reid

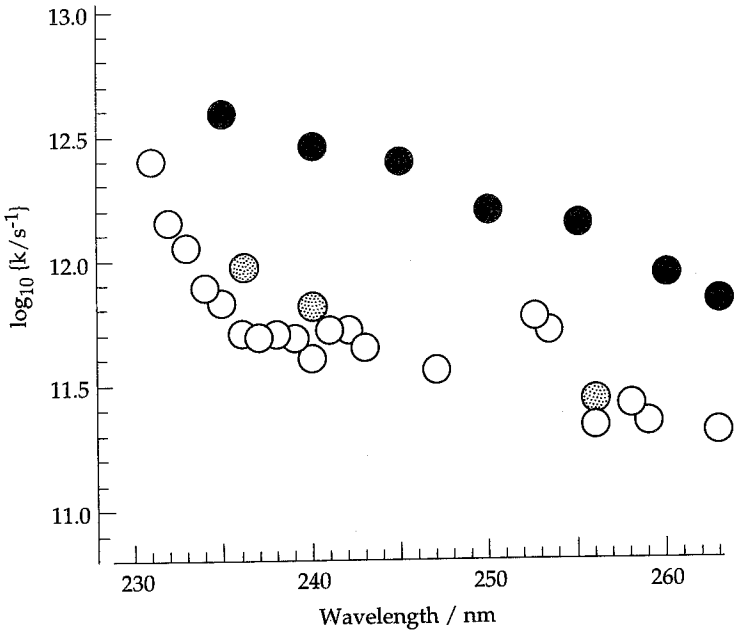

Figure 3-6. Rate coefficients $k(E)$ for $HOCO^{\dagger}$ decomposition. The filled circles are from Ionov et al. (1992, 1993b), who monitored all OH ($v = 0$) rotational levels. The open and shaded circles are from Scherer et al. (1990) (i.e., values of τ_2^{-1}) for $N = 1$ and $N = 6$, respectively.

and Reisler 1994; Reisler et al. 1994). Likewise, Moore and coworkers have observed fluctuations in $k(E)$ for the case of H_2CO unimolecular decomposition, again related to the sparseness of the manifold of parent energy levels (Hernandez et al. 1993; Miller et al. 1990).

It must be emphasized that such phenomena are to be expected for a statistical system only in the regime of low level densities. Theories like RRKM and phase space theory (PST) (Pechukas and Light 1965) are applicable when such quantum fluctuations are absent: for example, due to a large density of states and/or averaging over experimental parameter such as parent rotational levels in the case of incomplete expansion-cooling and/or the laser linewidth in ultrafast experiments. However, in the present case, it is unlikely that such phenomena can be invoked to explain why different rates are obtained when using ultrafast pump–probe methods that differ only in experimental detail.

The observed differences in the OH buildup rates at a given photolysis wavelength can be attributed to OH rotational levels having different parentages. For example, if higher-than-binary complexes yield mainly low N, this could be reflected in the product-state-selective measurements, even if the number of higher complexes is smaller than the number of binary complexes. In this case, there would be differences between results obtained with product state resolution versus those obtained by using a broadband probe. The latter would only be sensitive to the low N contribution in direct proportion to its fraction of the total product

yield, whereas spectral resolution enables the low N component to be isolated. A hypothetical situation is depicted in Figure 3-7 for two production mechanisms that yield cold and hot rotational distributions. Note that although the filled-bars contribution accounts for only 25% of the total population, it accounts for 80% of the $N = 1$ signal. Clearly, product spectral resolution offers a valuable addition to time domain studies when both can be used simultaneously.

To test for the possible participation of higher-than-binary complexes, Ionov et al. (1992, 1993b) recorded OH buildup times for different expansion conditions, that is, covering the range from modest to considerable clustering. The observed buildup times for a given photolysis wavelength did not change, even when clustering was so severe that the OH LIF signal level dropped. Our interpretation is that higher-than-binary complexes inhibit reaction and/or yield the same rates as do binary complexes. Inhibition is deemed most likely, since the reaction is quite endoergic and the gas phase cross section is known to be small near the thermodynamic threshold, increasing sharply only at significantly higher energies, as shown in Figure 3-8 (Chen et al. 1989). With its high entrance barrier, the $H + CO_2$ system is somewhat unique in this regard. In general, it is expected that the product buildup rate will depend on the size of the cluster. Additionally, as was the case in the nanosecond resolution experiments, variations of mass spectrometer signals at the mass of the mixed binary cluster versus OH LIF signal intensities were seen to be linear—a result that is pleasing but not conclusive. As will be discussed in section 3.4, double resonance selection of binary complexes will enable contributions from higher complexes to be eliminated. This will provide benchmark cases against which theoretical calculations can be tested. Also, by exploiting OH detection via LIF *as well as* H atom detection via the high-*n* Rydberg time-of-flight (HRTOF) method (Ashfold et al. 1992; Schneider et al.

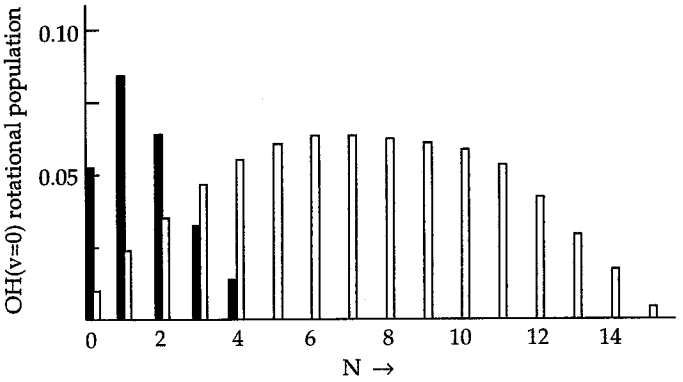

Figure 3-7. Hypothetical situation in which two distinct mechanisms yield hot and cold OH rotational distributions (open and filled bars, respectively). Though the open and filled bars represent 75% and 25%, respectively, of the total OH, the filled bar dominates at $N = 1$. Thus, state specific detection of $N = 1$ senses the minor channel in preference to the major channel. This might occur when two pathways yield hot and cold OH, for example, Br + $HOCO^{\dagger}$ versus $HO(Br)CO^{\dagger}$, respectively.

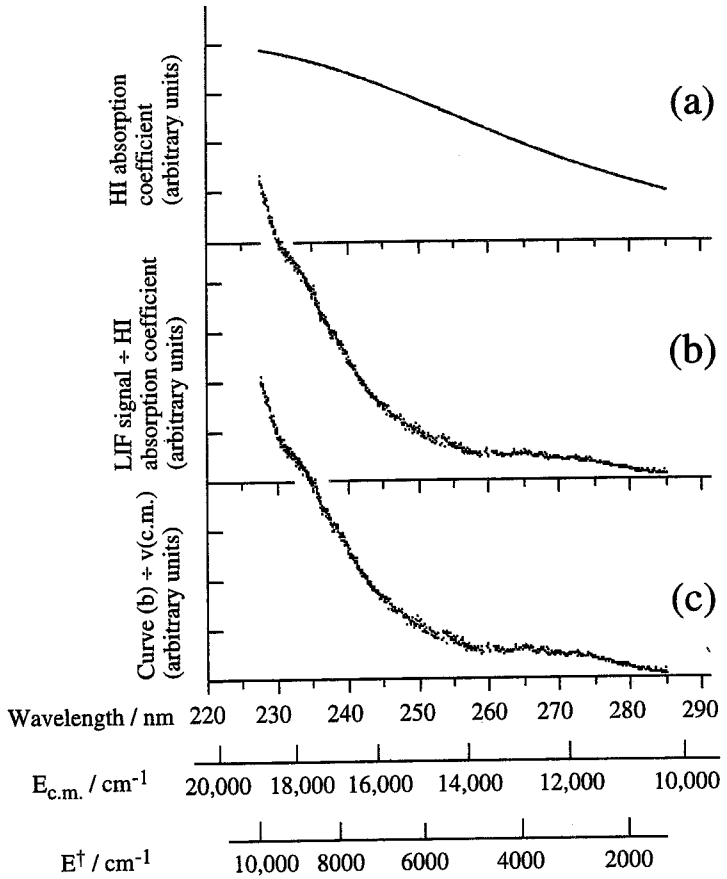

Figure 3-8. Production of OH versus photolysis wavelength for room temperature CO_2/HI samples (from Shin et al. 1991a): (a) HI 300 K absorption coefficient (arbitrary units) versus wavelength; the I* contribution has been removed since there is no contribution from slow hydrogen associated with I*, (b) normalized OH LIF signals divided by curve (a), yielding relative OH ($v = 0$, low N) production rates, (c) curve (b) divided by $v_{c.m.}$, yielding relative OH ($v = 0$, low-N) reaction probabilities. Also shown are the c.m. collision energies and $HOCO^{\dagger}$ energies in excess of the reaction endoergicity. Note the small reaction probabilities for $E^{\dagger} < 2000\ cm^{-1}$. These data can be converted to absolute cross sections by using the values obtained by Wolfrum and coworkers (e.g., 0.4 Å^2 at a collision energy of 15,000 cm^{-1}) (Jacobs et al. 1994).

1990; Wen et al. 1994), it will be possible to measure the reaction probability. Such a feat has not yet been accomplished.

Quite recently, time resolved measurements were carried out with complexes formed by expanding N_2O/HI/He mixtures (Ionov et al. 1994), where the reaction of interest is (Böhmer et al. 1992; Marshall et al. 1987, 1989):

$$H + N_2O \rightarrow OH + N_2 \qquad \Delta H = -63\ \text{kcal mol}^{-1}. \tag{2}$$

This system had been studied previously under gas phase, single-collision conditions, where it was shown that the dominant reactive pathway yields OH + N_2 via a 1,3-hydrogen shift mechanism (Böhmer et al. 1992). Specifically, by recording OH Doppler profiles, the N_2 product was found to contain a very large amount of internal excitation, which could be reconciled by assuming that hydrogen attaches initially to the terminal nitrogen and the $HNNO^{\dagger}$ intermediate thus formed then transfers the hydrogen to the oxygen via a transition state having a long N–N bond. Figure 3-9 shows the N_2 vibrational distribution calculated using a simple Franck–Condon model and a mean N–N separation of 1.23 Å, that is, the 1,3-hydrogen shift transition state value (Walch 1993). The fit to the OH sub-Doppler resolution lineshape is very good. We are aware of no other mechanism that can account for this high degree of N_2 internal excitation.

With complexes, reaction (2) was shown to be overwhelmingly dominant over the endoergic NO + NH channel (Hoffman et al. 1989a,b; Shin et al. 1992). Specifically, at the 255 nm photolysis wavelength of the time resolved measurements, the contribution from the NH + NO channel lies between the detection limit. It was our belief that participation of the $HNNO^{\dagger}$ intermediate *might* yield measurable OH production times (i.e., >100 fs).

As in the case of CO_2–HI, OH buildup rates were monitored as the degree of complexation was varied. However, this time a clear variation was observed in which the OH buildup time increased monotonically with the degree of complexation, as shown in Figure 3-10. This observation can be interpreted straightforwardly: whereas higher-than-binary complexes strongly inhibited reaction in the case of H + CO_2, reaction is less inhibited in the case of H + $N_2O \rightarrow$ OH + N_2, with its smaller entrance barrier. In the latter case, slowing of the H atoms does not inhibit reaction, while the increased heat capacity of the larger complexes results in smaller rates. Such conclusions are reasonable, but the evidence is circumstantial. Unequivocal proof is needed.

Participation of an $HO(X)CO^{\dagger}$ intermediate can also account for the observation that different OH rotational levels display different production rates, since this intermediate might yield rotationally cold OH via stepwise decomposition processes:

$$CO_2\text{–}HX + h\nu \rightarrow HO(X)CO^{\dagger} \rightarrow X + HOCO^{\dagger} \quad (3a)$$

$$\rightarrow XCO + OH \quad (3b)$$

$$\rightarrow HOX^{\dagger} + CO, \quad (3c)$$

followed by OH formation via decomposition of vibrationally excited $HOCO^{\dagger}$ and $HOX^{\dagger}$ deriving from reactions (3a) and (3c):

$$HOCO^{\dagger} \rightarrow OH + CO \quad (3d)$$

$$HOX^{\dagger} \rightarrow OH + X. \quad (3e)$$

Figure 3-11 provides a schematic description of these processes for the case of CO_2–HBr.

It was decided that the best way to examine this possibility was by carrying out electronic structure calculations for CO_2–HBr complexes in the ground and

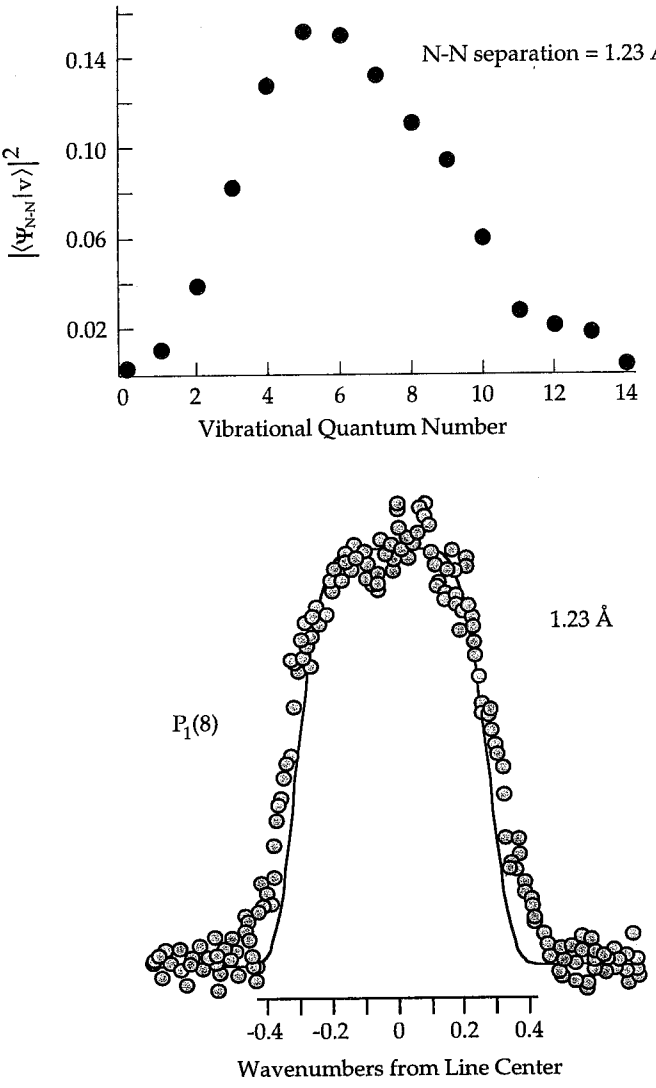

Figure 3-9. Sub-Doppler resolution OH LIF spectra indicate a modest amount of c.m. translational energy for all of the OH levels monitored in the reaction $H + N_2O \rightarrow OH + N_2$; see Böhmer et al. (1992) for details. A Franck–Condon projection of the 1,3-hydrogen shift transition state N–N separation of 1.23 Å (solid line, lower part) predicts a high degree of N_2 vibrational excitation (upper part) and yields good agreement with the data (shaded circles, lower part).

photoexcited states (Shin et al. 1991b). The motivations were: (1) to examine the possible role of the $HO(Br)CO^{\dagger}$ intermediate formed by simultaneous O–H and C–Br bond formation during HBr dissociation, (2) to obtain approximate wavefunctions for the intermolecular degrees of freedom and to use these to estimate the distribution of hydrogen approaches, and (3) to estimate the extent of the squeezed atom effect. Computational details are given elsewhere (Shin et al.

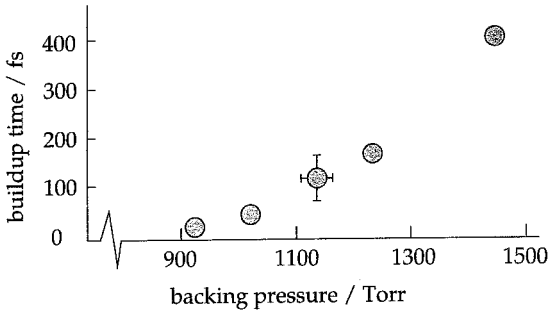

Figure 3-10. Ultrafast pump–probe measurements with supersonically expanded $HI/N_2O/He$ mixtures show that OH buildup times vary with the degree of complexation. At the lowest backing pressures, the buildup times are ≤ 100 fs. For buildup times below 100 fs, the uncertainties associated with fitting the data to assumed lifetimes are too large to allow other than an upper limit to be obtained.

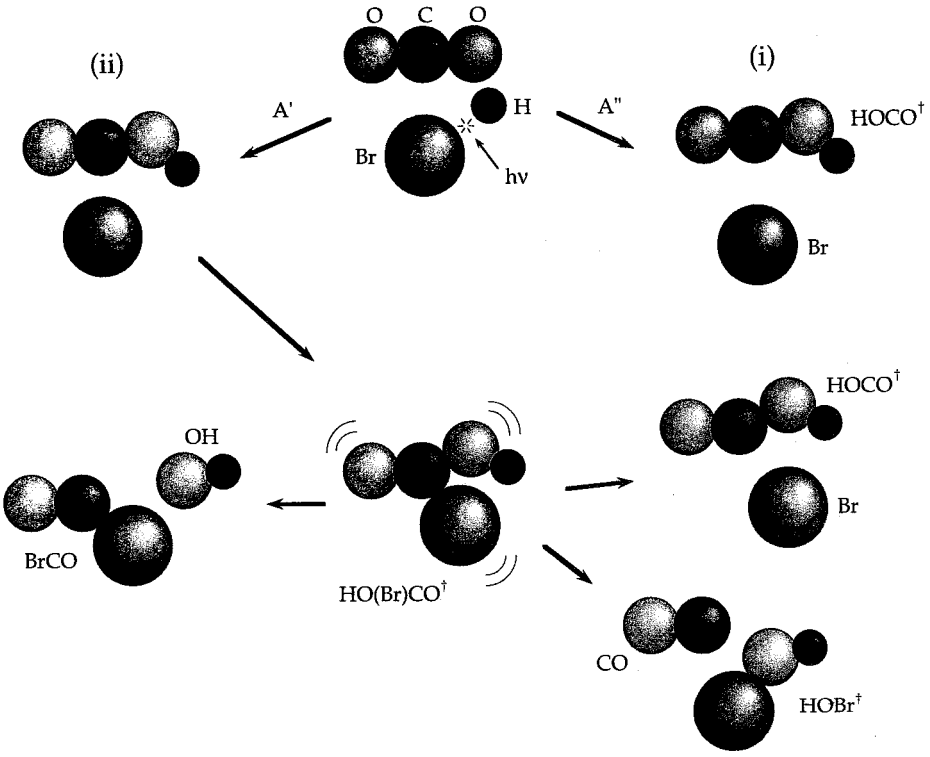

Figure 3-11. Schematic representation of CO_2–HBr photoexcitation proceeding via A′ and A″ PESs, neglecting spin–orbit interaction. There is no C–Br bonding on the A″ surface and the system evolves to $HOCO^{\dagger}$ and Br moving away from each other as per the squeezed atom effect, as depicted in (i). The A′ surface supports weak C–Br bonding that can evolve to a vibrationally excited $HO(Br)CO^{\dagger}$ intermediate, as depicted in (ii), which can decompose via several channels; see text for details.

1991b); the methodology employed was that developed over many years by Goddard and coworkers.

In the case of (1), it was found that both attractive and repulsive C–Br interactions were possible, depending on the orientations of the bromine orbitals (i.e., A′ versus A″, respectively). Our original intuition was that hydrogen capture might be facilitated by the presence of the C–Br interaction, due to rehybridization of the orbitals on the carbonyl. This turned out to be a small effect because of the initial geometry afforded by the weakly bound precursor. The attractive C–Br interaction was found to be only $\sim 170\ cm^{-1}$ at the 3.6 Å C–Br distance of the weakly bound precursor, as shown in Figure 3-12. Nonetheless, C–Br attraction can facilitate the formation of a highly excited $HO(Br)CO^{\dagger}$ intermediate whose decomposition is expected to be dominated by the $Br + HOCO^{\dagger}$ and/or $CO + HOBr^{\dagger}$ channels. The $HOCO^{\dagger}$ and/or $HOBr^{\dagger}$ thus produced may account for OH product being formed with low N and with longer buildup times than OH deriving from $HOCO^{\dagger}$ formation that occurs without the participation of the $HO(Br)CO^{\dagger}$ intermediate.

In the case of (2), it was found that several percent of the hydrogen atoms make approaches that have high reaction probabilities. The angular potential is very shallow (see Figure 3-13), thus accommodating large amplitude zero point fluctuations, and Schatz has shown that many of these are likely to have appreciable reaction probability (Schatz and Fitzchartes 1988). This confirmed our intuition, but did little to improve our understanding. In the case of (3), it

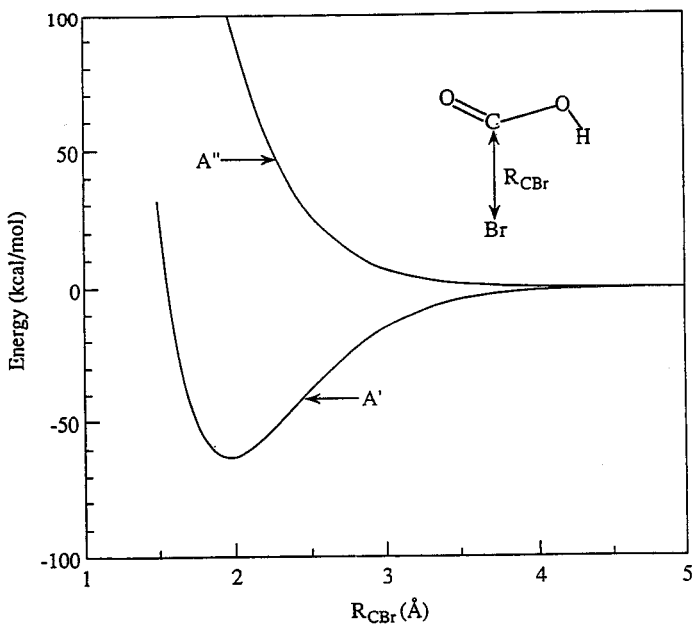

Figure 3-12. Calculated potentials for A′ and A″ PESs versus C–Br distance, showing the repulsive and attractive natures of these surfaces; from Shin et al. (1991b). Note that the C–Br distance in CO_2–HBr is 3.6 Å (Sharpe et al. 1990; Zeng et al. 1992).

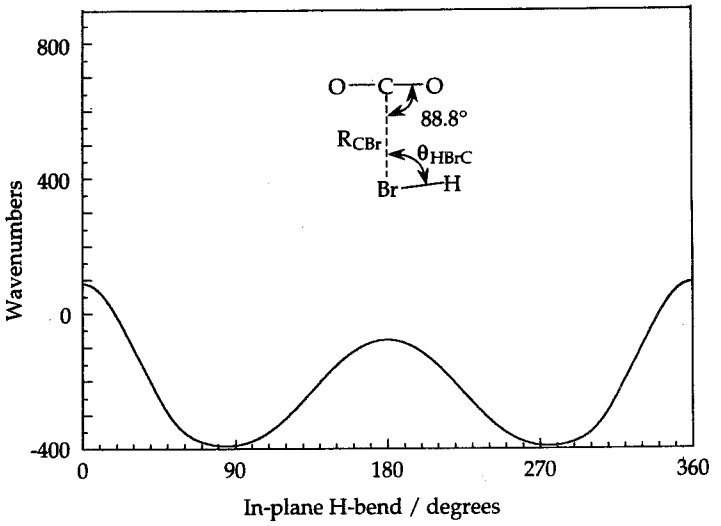

Figure 3-13. Optimized reaction path for in-plane hydrogen motion, showing the shallowness of the potential which gives rise to large amplitude zeropoint fluctuations.

was shown that the potential energy along the direction of hydrogen departure was consistent with what one would expect for the degree of Br–HOCO recoil inferred from the experiments.

The above calculations, in which the possible participation of a $HO(Br)CO^{\dagger}$ intermediate was confirmed, provide a means of reconciling the different rate measurements. For example, with equal A′ and A″ photoexcitation yields, $HO(Br)CO^{\dagger}$ can be formed as much as half the time. However, this is an upper limit, and it is more likely that $HO(Br)CO^{\dagger}$ is formed less than half the time. If these intermediates contribute rotationally cold OH, for example, via reactions (3d) and (3e), the spectrally resolved observation of OH ($N = 1$) can yield longer lifetimes than the measurements in which all rotational levels are probed simultaneously. This explanation is consistent with all of the experimental observations. However, though it *can* reconcile the Scherer et al. and Ionov et al. rate measurements, we emphasize that proof is still needed.

3.2.5. Theoretical Modeling of the Reaction Dynamics

For single-collision conditions (i.e., no complexes), this system has been examined at levels of dynamical theories ranging from classical trajectories (Kudla and Schatz 1991; Kudla et al. 1991, 1992; Schatz 1989) to quantum scattering (Clary and Schatz 1993; Schatz and Dyck 1992), and resonance stabilization (Hernández and Clary 1994). As long as the PES is good, the trajectories should give reasonable values for the reaction rates (i.e., within a factor of 2 or 3) at the experimental energies of the hot atom reactions, which lie well above the threshold region. This seems to be the case, though when using classical mechanics with an imperfect

PES it is hard to assign fault uniquely when the calculations fail to reproduce accurately the known facts.

Since there are only four atoms, this case can act as a useful bridge between classical and quantum dynamics calculations. Since nonadiabatic effects are expected to be minor, the quantum calculations are limited by the PES and the computational precision. Consequently, they will ultimately offer the most meaningful comparison between experiment and theory. However, the quantum dynamics calculations carried out to date have been limited to two dimensions. Therefore, they have little to do with the HOCO system per se, except in the general sense of exploring the physics of vibrational resonances coupled to continua.

Our belief is that $k(E)$ can be predicted for $HOCO^{\dagger}$ decomposition reasonably well by using RRKM theory. Though not intellectually appealing, this is expected to yield good numbers. Since $k(T)$ has been fitted over the temperature range $80 \leq T \leq 2000$ K, the use of RRKM theory amounts to essentially an extrapolation of known rates to the higher energies that are accessed in the hot atom experiments. This is the reason that the RRKM approach is presently the most accurate; that is, it is a representation of reliable experimental rate data over a range of temperatures. Caveats about IVR time scales, etc., limit the accuracy and useful range of the extrapolation, but do not change this conclusion.

With complexes, the only dynamical calculations to date have been classical trajectories in which it was assumed that there is no significant C–Br chemical interaction following photoexcitation (Schatz and Fitzcharles 1988). Consequently, the role of the complex has been limited to $H + CO_2$ interactions sampled over the probability density for the intermolecular degrees of freedom, as well as the squeezed atom effect. These calculations have yielded reaction probabilities versus attack angle and nascent V, R, T excitations which are in reasonable agreement with the experimental results. Much work is still needed and the challenges are daunting.

3.3. THE REACTION $Br + I_2 \rightarrow IBr + I$ VIA THE WEAKLY BOUND $HBr–I_2$ PRECURSOR

In section 3.2, experiments were described in which photodissociation of the HX moiety within a weakly bound complex liberated hydrogen atoms which then went on to react with the other moiety in the complex. Alternatively, photodissociation of HX moieties within weakly bound complexes can be used to prepare halogen atom reactants. This provides advantages which derive mainly from the rapid removal of the hydrogen.

In the first demonstration of this approach, Sims et al. photodissociated HBr within $HBr–I_2$ complexes in order to initiate the reaction (Gruebele et al. 1991; Sims et al. 1992):

$$Br + I_2 \rightarrow IBr + I \qquad \Delta H = -6.7 \text{ kcal mol}^{-1} \tag{4}$$

where reaction is believed to transpire via a long-lived $Br–I–I^{\dagger}$ intermediate. This and similar reactions involving three halogen atoms have served as valuable

prototypes since the early days of reaction dynamics (Beck et al. 1968; Blais and Cross 1970; Carter et al. 1973; Cross and Blais 1969, 1971; Firth and Grice 1987a,b; Firth et al. 1987a,b; Fisk et al. 1967; Girard et al. 1987, 1991; Hoffmann et al. 1983; Lee et al. 1968, 1969, 1977; Loesch and Beck 1971; Trickl and Wanner 1983). Specifically, a number of groups have demonstrated the important role played by the trihalogen intermediate, mainly by using the crossed molecular beams technique. In these studies, it was possible to infer the lifetime of the intermediate only indirectly, that is, by comparing the observed angular distribution in the c.m. system to calculations that require, as input, an estimated average rotational period (Lee et al. 1968). However, by exploiting the $t = 0$ clocking method, Sims et al. were able to obtain the IBr buildup time directly. In the absence of processes additional to reaction (4), this is the same as the Br–I–I† decomposition lifetime.

Although the structure of the HBr–I_2 complex has not yet been determined experimentally, it seems probable that the hydrogen faces outward (Sims et al. 1992). For example, the analogous cases of HF–ClF and HF–Cl_2 have been examined by Klemperer and coworkers who used the molecular beam electric resonance technique to determine the average structures (Baiocchi et al. 1982; Novick et al. 1977). In both cases, the three halogen atoms were found to lie along a straight line. For HF–ClF, they deduced an average H–F–Cl angle of 125° for both the deuterated and undeuterated cases, and from this they concluded that the H–F–Cl equilibrium angle is $\sim$125°, albeit with a large hydrogen zero point amplitude. Recently, Blake and coworkers examined HF–Cl_2 and found it to be quasilinear (Stockman and Blake 1993).

With the hydrogen facing outward, its role differs qualitatively from the case of CO_2–HX complexes. Namely, HBr photodissociation ejects the hydrogen *away from* the I_2, while giving the Br atom a modest push *toward* the I_2, as shown in Figure 3-14. This rapid ejection of ejection of hydrogen places the system on the triatom PES near the linear geometry, whereas the equilibrium angle is expected to be $\sim$150° with a small barrier to linearity (Sannigrahi and Peyerimhoff 1986; Viste and Pyykkö 1984). Reaction follows, unaffected by the hydrogen which has long since departed. This system is clean experimentally in the sense that the hydrogen atom leaves on a time scale that is nearly two orders of magnitude shorter than that of the subsequent dynamics. Note that this is true regardless of the dynamical details of how the hydrogen escapes.

The photodissociation of uncomplexed HBr leaves the Br atom in one or both of the spin–orbit states (i.e., the $^2P_{3/2}$ ground state and the $^2P_{1/2}$ excited state, hereafter referred to as Br*) with relative populations that depend on the photolysis wavelength (Magnotta et al. 1981; Xu et al. 1987, 1988). With HBr–I_2 complexation, rapid hydrogen departure places the trihalogen system at a geometry in which the Br–I_2 distance is large and Br–I_2 attraction is weak relative to the bromine spin–orbit splitting. Thus, the system begins evolving on potentials which, to a first approximation, preserve the Br and Br* atomic spin–orbit electronic configurations in the entrance channel. For Br* it is unlikely that direct reactive channels are open, since it has been shown that a propensity exists in which spin–orbit excitation is preserved in such trihalogen exchange reactions (Gordon et al. 1982; Haugen et al. 1985; Hofmann and Leone 1978; Wiesenfeld and Wolk 1978a,b). Indeed, the reaction I* + Br_2 → IBr + Br* even leads to a

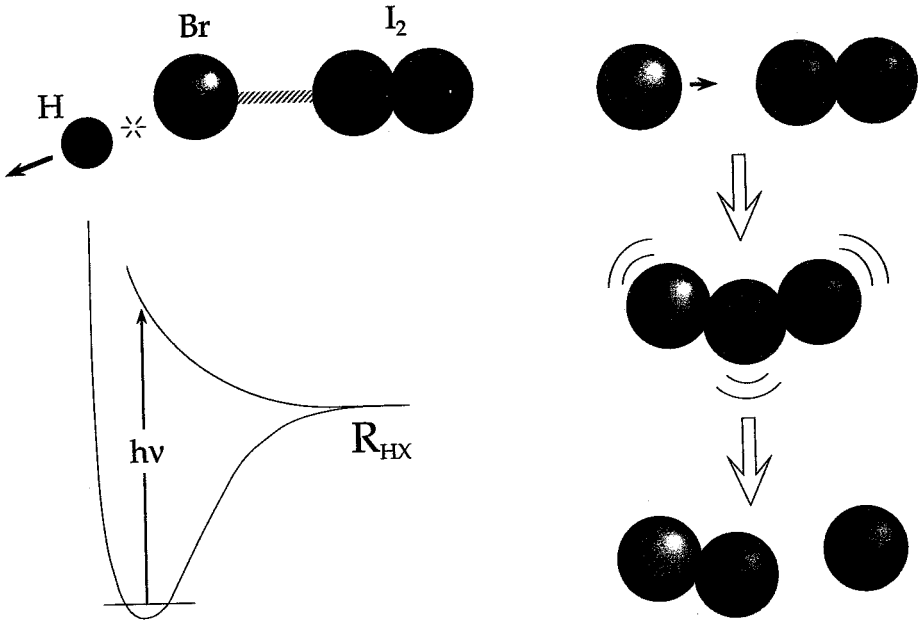

Figure 3-14. Schematic drawing of the photoinitiated reaction of Br with I_2. Hydrogen removal is rapid, relative to the characteristic time scales of the motions of the heavier nuclei. Photoexcitation at 220 nm yields primarily $Br(^2P_{3/2})$, though some $Br(^2P_{1/2})$ is also produced. As shown on the right, reaction transpires via the vibrationally excited trihalogen intermediate.

population inversion and consequent laser oscillation on the Br ← Br* transition at 3685 cm^{-1} (Spencer and Wittig 1979). The main participation of Br* in producing IBr is expected to be due to quenching of Br* followed by reaction (4).

The distribution of orbital alignments and orientations relative to the I_2 moiety are dictated by the zero point distribution of HBr axes in the weakly bound precursor. It is reasonable to assume that this distribution of HBr axes results in an effective Br–I_2 long range potential which is less attractive than for the most favorable orbital arrangement. This brings up a valuable aspect of this approach, namely, that the trihalogen system begins its life on a long-range part of the PES, which is one of the hardest regions to study, both experimentally and theoretically. Since observables such as rates can depend sensitively on this part of the PES, it is possible that the elusive long-range interaction problem can be addressed. Consequently, while important in its own right because of the scientific significance of the trihalogens, this experiment also opens the door to complementary studies.

In the experiments of Sims et al., it was found that IBr was formed with a risetime of 53 ± 4 ps when photolyzing HBr–I_2 complexes at 218 nm. A typical experimental trace is shown in Figure 3-15 (lower trace). In this case, the Br + I_2 "collision energy" in the c.m. system is 145 cm^{-1}, neglecting the van der Waals interaction in the entrance channel. A similar result (44 ± 4 ps) was obtained with DBr–I_2 (upper trace), for which the collision energy is 286 cm^{-1}. Assuming that most of the observed IBr derives from Br rather than Br* photoproducts, these

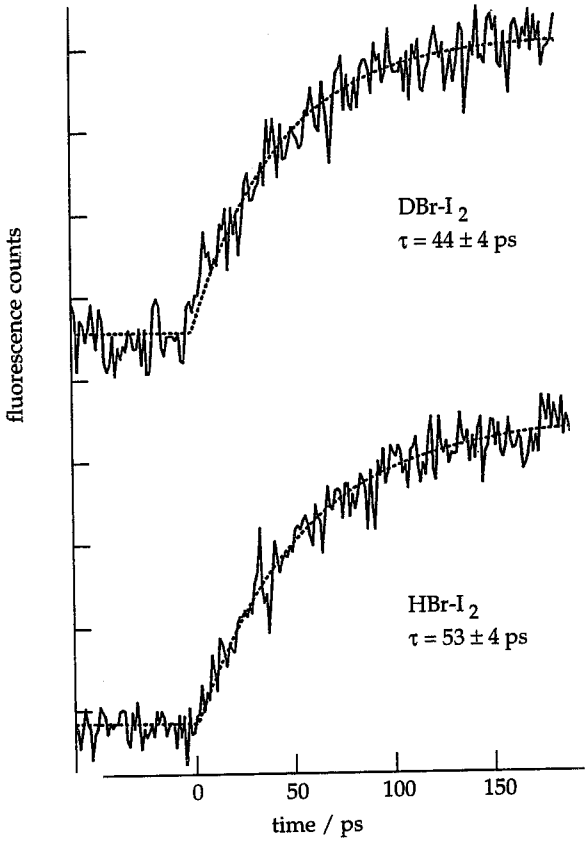

Figure 3-15. Typical experimental traces showing IBr buildup following 218 nm photoexcitation of $HBr–I_2$ and $DBr–I_2$ complexes.

data confirm the long IBr buildup times that result from the presence of a significant well along the reaction coordinate. Moreover, they support the contention that the hydrogen faces outward; otherwise, the opposite trend would be expected, that is, a longer lifetime for $DBr–I_2$ than $HBr–I_2$.

The van der Waals attraction between Br and I_2 is estimated to be $\sim 400\ cm^{-1}$ by analogy with halogen/rare gas complexes (Bieler and Janda 1990; Bieler et al. 1991). This ensures that photodissociation of the HBr moiety cannot produce Br + I_2 except via quenching of Br* or the unlikely instance in which the hydrogen is trapped efficiently between the heavy particles. With the Br atom unable to escape from the I_2 because of the $Br–I_2$ van der Waals attraction, the system is ensured of an essentially unity quantum yield.

It was possible to construct a PES which was consistent with the earlier work on trihalogens and which was able to reconcile the main findings of the time resolved studies by using the method of classical trajectories (Sims et al. 1992). A range of parameters was explored, and the experimental results were reproduced best by using wells lying 13–17 kcal mol^{-1} below the entrance channel with exit barriers of 3–4 kcal mol^{-1}. A schematic energy diagram is shown in

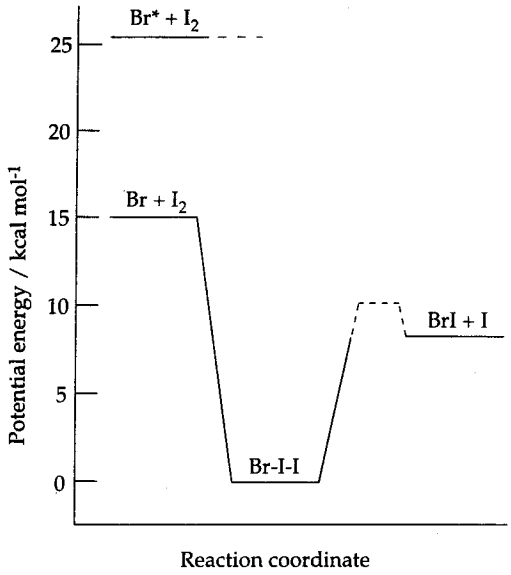

Figure 3-16. Partial energy diagram for the Br + I_2 system. The Br($^2P_{1/2}$) is not expected to react directly, though reaction can occur following quenching to Br($^2P_{3/2}$).

Figure 3-16. Minor changes in the parameters that define the PES did not result in large differences in calculated lifetimes, for example, approach angles of 0° (collinear) and 55° gave results that differed by only 20%, with 0° yielding the smaller lifetimes. The conclusion is that a qualitatively intuitive PES with a well lying ~ 15 kcal mol^{-1} below the entrance channel and ~8 kcal mol^{-1} below the exit channel can reconcile the main experimental finding of a lifetime of ~50 ps for the Br–I–I^+ intermediate. The exit barrier of 3–4 kcal mol^{-1} provided the best fit, but since nuances such as the van der Waals interaction in the entrance channel were suppressed, this should be viewed as providing grist for further theoretical work. For example, recall that the measured lifetimes for the 145 and 286 cm^{-1} "collision energies" are 53 ± 4 ps and 44 ± 4 ps, respectively. Likewise, computational results for the 145 cm^{-1} collision energy yielded consistently longer lifetimes (30% on average) than those obtained with the 286 cm^{-1} collision energy. Consequently, the inclusion of the Br–I_2 van der Waals attraction into the trajectory calculations is expected to lengthen the lifetime by starting the reaction at a lower energy, thereby lessening the size of the exit barrier needed to fit the data.

Recently, Wright et al. (1994) used ultrafast photoionization techniques to detect vibrationally excited I_2 following 220 nm photoexcitation of HBr–I_2 complexes. They attributed this to quenching of Br* by I_2, pointing out that their measured lifetime of 51 ± 5 ps is close to those reported by Sims et al. (1992). This raises exciting possibilities. It seems inevitable that Br*–I_2 complexes will find their way eventually to the ground state PES since there is nowhere else to go. However, although the Br* yield at 220 nm is unknown, it is expected to be modest. Specifically it is only 15% at 193 nm and is expected to diminish at

longer wavelengths (Magnotta et al. 1981; Xu et al. 1987, 1988). Thus, if the Br* photoproduct proves to be the main source of IBr, this implies that there is a barrier in the entrance channel for the $Br + I_2$ reaction. Given the delicate interplay between the atomic halogen spin–orbit interaction and the forces present in the region of the triatom well, it will be important to examine this system in more detail.

Finally, we wish to point out that the modest well depth of the $Br–I–I^{\dagger}$ intermediate places this system in the category of a unimolecular decomposition reaction in the limit of a low density of states. This is not unlike the case of NO_2, which has received considerable attention (Hunter et al. 1993; Peskin et al. 1994; Reid et al. 1993a,b; Reid and Reisler 1994; Reisler et al. 1994). In such cases, the rates are expected to fluctuate as per the overlap of the wavefunctions of the $Br–I–I^{\dagger}$ resonances with those of the IBr + I exit channel continuum, with chaotic mixtures of the continuum contributions. The manner in which the experiments are carried out leads to some averaging over $Br–I–I^{\dagger}$ rotational levels and total energies, but this may not wash out the fluctuations in rates that occur as the energy is tuned. Therefore, it will be very useful to extend the rate measurements to cover a continuous range of photon energies. Additionally, small characteristic rates like those observed ($2 \times 10^{10}\ s^{-1}$) raise the spectre of observing step-like structure in $k(E)$, corresponding to the successive openings of reactive channels. These have been observed in photoinitiated reactions of H_2CO (Lovejoy et al. 1992) and NO_2 (Brucker et al. 1992; Ionov et al. 1993a; Miyawaki et al. 1990, 1991, 1993; Wittig and Ionov 1994) and can be assigned to quantized features of the transition state. With the trihalogens, such steps would reveal dynamical features that have yet to be observed under scattering conditions, despite numerous predictions (Chatfield et al. 1991a,b, 1992a,b, 1993; Friedman and Truhlar 1991; Lynch et al. 1991; Truhlar et al. 1990).

3.4. PROSPECTS FOR FUTURE RESEARCH

Many factors and considerations are germane to future research in this area. On the technical side, achieving cluster size selection stands as one of the most important and sought-after goals. It would be most desirable to achieve this while maintaining sufficiently high densities for studies of photoinitiated reactions to be carried out with product state resolution and/or ultrafast time resolution. The two methods that, in our opinion, are most viable are molecular beam deflection, as pioneered by Buck (1994) and coworkers, and laser-based double-resonance methods. Less direct approaches are deemed inferior.

The molecular beam deflection method is shown schematically in Figure 3-17 (Buck et al. 1985). It is based on momentum transfer between clusters entrained in a molecular beam and rare gas atoms which are the constituents of a second molecular beam at 90° to the cluster beam. Collisions between the rare gas atoms and the clusters under single-collision conditions deflect a small percentage of the clusters from their original path. The maximum deflection angle depends on the mass of the cluster. For example, binary clusters may be deflected into a broad range of angles with a well defined upper limit set by the momentum conservation

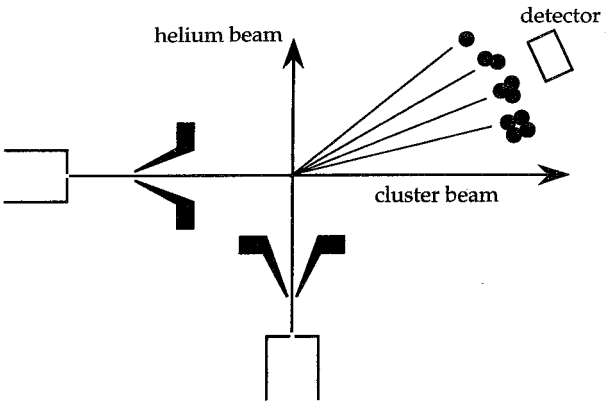

Figure 3-17. Schematic of the molecular beam deflection method. Under single-collision conditions, collisions between clusters and He atoms deflect the clusters to angles whose maxima are determined by momentum conservation.

condition, while higher clusters are scattered into narrower ranges of angles. As the number of subunits in the cluster increases, the upper limits to the deflection angle decrease successively.

Since the present experiments that use this approach employ mass spectrometric detection, it is essential that the neutral cluster of interest yields a signal at the parent mass. It is not problematic if ion fragmentation in the mass spectrometer is severe, as long as the neutral clusters yield enough ions at the parent masses to provide acceptable count rates. In this case, the cluster ion signal at the maximum-allowed deflection angle is a faithful signature of the neutral cluster. Higher clusters may fragment severely in the ionizer of the mass spectrometer, yielding large ion concentrations at the mass of interest; however, these higher clusters will be deflected to smaller angles than the neutral cluster having the same mass as that monitored mass spectrometrically.

This method of separating clusters has become an important experimental technique which has been applied to the study of several important classes of clusters: van der Waals (e.g., ethylene) (Alrichs et al. 1990; Buck et al. 1987, 1988c), dipolar (e.g., acetonitrile) (Buck 1992; Buck and Ettischer 1994; Buck et al. 1990a), and different hydrogen bonds (e.g., ethylene–acetone) (Buck et al. 1993) and isomers have also been identified (e.g., methanol versus hydrazine) (Beu et al. 1994; Buck et al. 1988a,b, 1990b,c; Huisken et al. 1991; Huisken and Stemmler 1988, 1992). It can be used with mixed clusters (e.g., methanol hexamer) (Buck et al. 1990b; Buck and Hobein 1993). Moreover, it is very general. It can be applied to almost any species and is generous in the range of cluster sizes that can be accommodated. An example from the work of Buck and coworkers is given in Figure 3-18 showing the time dependence used to identify different clusters (Buck et al. 1985).

One of the disadvantages is that the clusters thus separated have internal excitations. This can be detrimental in cases where one would like to use the clusters after they have been separated, particularly if it is desirable to maintain, to the extent possible, a well defined geometry. Even at 0 K, large zero point

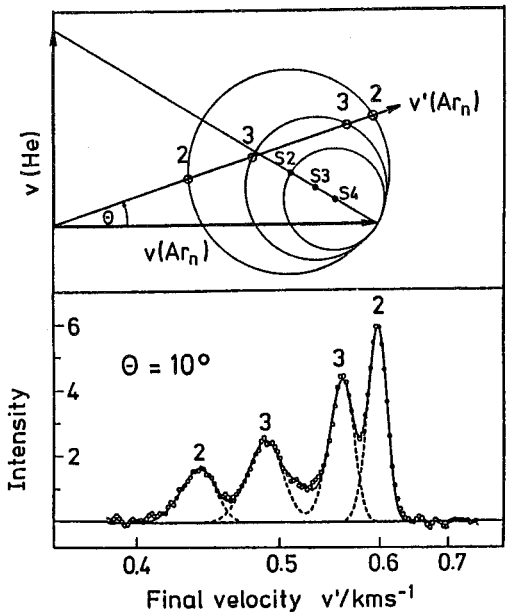

Figure 3-18. Experimental demonstration of the molecular beam deflection method, from Buck et al. (1985). The Newton circles show the peak positions associated with the different clusters; S_i denotes the velocity of the center-of-mass for different clusters. The TOF data were recorded at a lab angle of 10°; note the correspondence between peaks 2 and 3 and the corresponding intersection points on the Newton circles.

amplitudes preclude the possibility of assigning the "geometry" to the equilibrium value, and excitation of intermolecular vibrations exacerbates this problem severely. For example, a modest amount of vibrational excitation in the internal degrees of freedom can cause the cluster to have liquid-like behavior (Buck 1994). Moreover, this problem is most severe for small clusters when using the molecular beam deflection method.

Another disadvantage is that, though certain spectroscopic studies can be carried out with the selected clusters, it is difficult to envision the present embodiment of this method as providing high enough concentrations of selected clusters to apply product-state-selective and/or ultrafast techniques to photo-initiated reactions within the selected complexes. This is because the process whereby the clusters are differentiated employs strong, momentum-changing collisions, that is, such collisions tag the clusters' translational degree of freedom. It is possible that a precision Doppler method could catch the clusters thus tagged before they disperse from the interaction region, but this has yet to be demonstrated. Once they have separated in space, the low concentrations that result make it difficult to use such selected clusters in further photochemical studies.

The Buck method is most useful for medium sized clusters, and in experiments that do not attempt detailed photochemical studies of the size selected clusters. High resolution spectroscopy of the selected clusters is impractical because the number per quantum state is small, due to the many occupied ro-vibrational

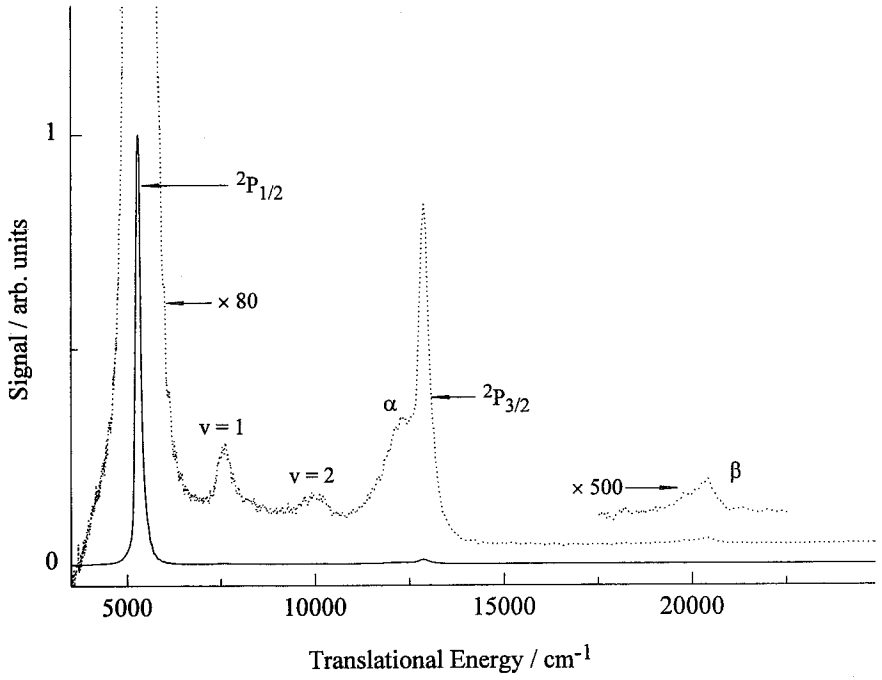
1
0
Signal / arb. units
$^2P_{1/2}$
× 80
v = 1
v = 2
α
$^2P_{3/2}$
× 500
β
5000
10000
15000
20000
Translational Energy / cm^{-1}

(a)

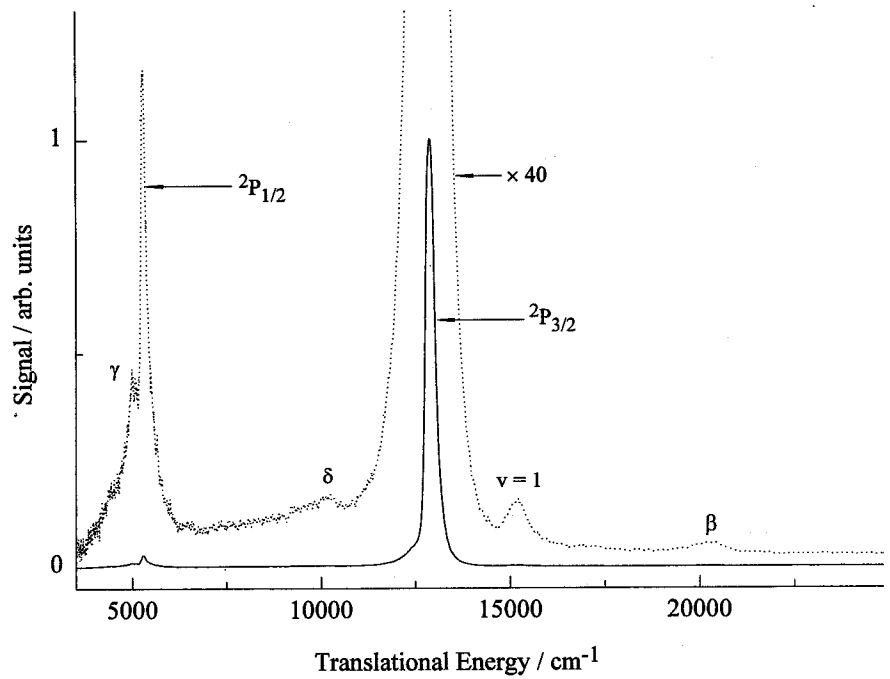
1
0
Signal / arb. units
$^2P_{1/2}$
γ
δ
× 40
$^2P_{3/2}$
v = 1
β
5000
10000
15000
20000
Translational Energy / cm^{-1}

(b)

levels. However, low resolution spectroscopic studies can be revealing (Buck 1994), though interpretation requires care.

At least for the near future, we believe that the method of choice for overcoming the size selection problem for binary complexes is double resonance photoinitiation using pulsed lasers—one operating in the infrared, the other in the ultraviolet. This is analogous the methods developed by Crim and coworkers (Brouwer et al. 1987; Butler et al. 1986; Crim 1984; Dübal and Crim 1985; Rizzo et al. 1983; Sinha et al. 1990; Tichich et al. 1986, 1987) and Rizzo and coworkers (Fleming et al. 1991a,b,c; Fleming and Rizzo 1991; Luo et al. 1990; Luo and Rizzo 1990, 1991). The infrared pulse tags complexes by exciting (primarily) a moiety whose ultraviolet absorption is red-shifted by virtue of the implanted vibrational excitation. This step is also innately state selective and, by using nanosecond lasers, rotational resolution of the complexes will usually be possible. In the presence of ultraviolet radiation, complexes thus tagged can experience two fates: (1) vibrational predissociation, yielding free molecules which, in general, will possess vibration and rotation excitation, and (2) photodissociation of one moiety within the complex, namely, the one containing the implanted vibrational excitation. With ultrafast lasers, there is a trade-off between vibrational predissociation and spectral resolution. To ensure the latter, one might choose transform-limited infrared pulses of ~ 100 ps duration, which is short enough to overcome most vibrational predissociation rates. This is compatible with the subsequent application of ultrafast pump–probe techniques.

With nanosecond lasers, predissociation rates are usually slow enough to permit individual rotational lines to be resolved, though they are often fast compared with typical pulse durations. Therefore, one must be wary of the possibility that vibrational predissociation removes most of the tagged complexes. For example, a homogeneous linewidth of only 30 MHz is sufficiently narrow that it may be hard to observe in spectroscopic studies, but could prove devastating were there a delay of tens of nanoseconds between the tagging and photodissociation pulses. Since it will not always be possible to determine predissociation lifetimes a priori, the recommended approach is to use temporally overlapped pulses and high ultraviolet intensities. In this case, the fate of the tagged complexes is determined by the relative rates of ultraviolet photoexcitation versus predissociation. Under optimal conditions, most of the tagged complexes will be further excited with the UV radiation with only a slight loss of spectral resolution due to the additional lifetime broadening caused by efficient up-pumping. Numerical estimates suggest that it will not be difficult to overcome subnanosecond predissociation lifetimes. For example, consider 266 nm HI photodissociation, for

Figure 3-19. Photodissociation of HI monomers and clusters. The solid traces indicate the substantial discrimination available when using polarized photolysis radiation; note the high S/N. Under conditions of such minimal clustering, it is reasonable to assume that most of the clusters are binary. Peaks labeled $v = 1$ and $v = 2$ are due to inelastic H + HI collisions within the cluster. The superelastic peak β is assigned tentatively to secondary photolysis of I*–HI complexes, in which the escaping hydrogen deactivates the nearby I*. (a) Vertical and (b) horizontal polarization of the photolysis radiation relative to the molecular beam. The plenum pressure is 1900 torr.

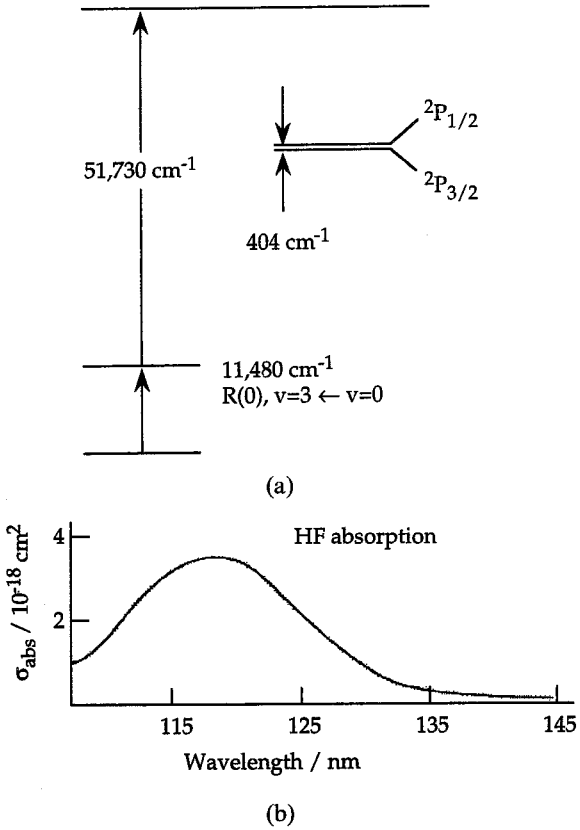

Figure 3-20. (a) Schematic of sequential two-photon HF excitation scheme and (b) HF absorption spectrum. Note that HF absorption above 150 nm (66, 700 cm^{-1}) is very weak; from Lee (1985).

which $\sigma_{abs} = 3 \times 10^{-19}$ cm^2. A 20 mJ pulse of 5 ns duration focused into a 0.1 mm^2 spot results in optical excitation rates $>10^9$ s^{-1}. Such experimental conditions are easily met, ensuring that a multitude of experiments are possible in the nanosecond regime.

Figure 3-19 shows an experimental result obtained by expanding HI/He mixtures under conditions that discriminate against higher-than-binary complexes (Segall et al. 1994). Of course, higher-than-binary clusters are present to some extent, but every effort was made to minimize their presence, namely, the very high S/N enabled the experiments to be carried out under conditions of minimal clustering.

In these experiments, there was no double-resonance tagging, so all of the HI moieties were available for photodissociation. What is observed experimentally is the resulting atomic hydrogen time-of-flight distribution which is obtained by using the HRTOF technique (Ashfold et al. 1992; Schneider et al. 1990; Wen et al. 1994). This method provides excellent resolution and S/N compared to other TOF methods. The dominant features (solid curves) are due to HI monomer. However, upon magnification, features are seen that are due to

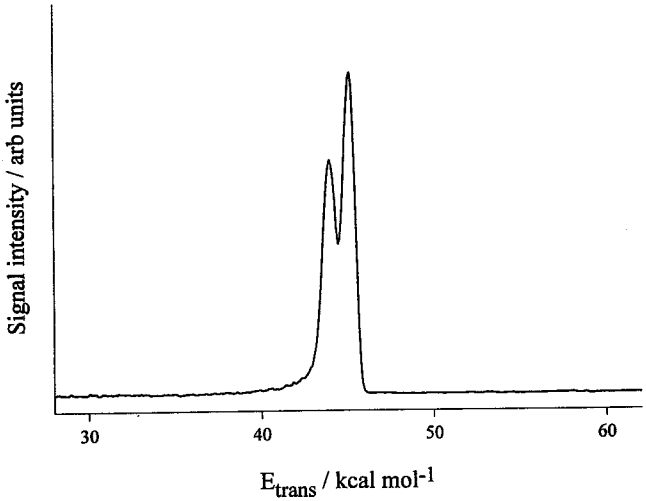

Figure 3-21. Experimental realization of the scheme given in Figure 3-20. The peaks correspond to the fluorine spin–orbit states. The low resolution relative to the data shown in Figure 3-19 is due to the large linewidth of the 193.3 nm excitation laser.

complexes. The photodissociation of an HI moiety in $(HI)_2$ produces HI in $v = 1$ and 2 via intracluster collisions of photolyfically produced hydrogen atoms with the nearby HI moiety. This inelastic process results from "missed reactions." In this example, the peaks labeled $v = 1$ and 2 derive from the photodissociation of the vibrationally excited HI which is produced by the first photochemical event in the $(HI)_2$ complex. It was verified by H → D substitution that the peaks shown in Figure 3-19 are due to HI vibrations, and the sequential two-photon nature of the $v = 1$ and 2 peaks was confirmed by fluence dependence measurements. Furthermore, there is a small feature which is offset from the monomer by approximately the iodine spin–orbit energy. This is assigned to the scattering of hydrogen from nearby I* that is produced by the first ultraviolet photon, deactivating the I* in the process.

It is noteworthy that the photolytic removal of the second hydrogen atom from the complex is quite efficient. Thus, even under "ordinary" experimental conditions, it will be possible to ensure efficient ultraviolet photoexcitation in the face of subnanosecond predissociation lifetimes.

The initial step in the double-resonance scheme is the excitation of a local mode hydrogen stretch vibration localized in a hydrogen halide moiety. In principle, this can be done either at the fundamental or one of the overtones. With presently available Ti:sapphire lasers and parametric oscillators (OPOs), it is possible to saturate fundamentals and first overtones, thus ensuring maximum population transfer. Second overtones cannot be pumped as efficiently, but offer enormous discrimination against background and can be used to shift frequencies out of the vacuum ultraviolet and into a more user-friendly part of the ultraviolet. Thus, first and second overtones are very attractive.

As with the HI example given above, a "demonstration of principle"

experiment is needed, and Figure 3-20 shows just this (Zhang et al. n.d). Hydrogen fluoride gas was cooled by supersonic expansion and the $\Delta v = 3$ R(0) transition was excited by using a narrow bandwidth pulsed Ti:sapphire laser. These molecules were photodissociated by using just a few millijoules of 193 nm radiation. The resulting hydrogen translational energy distribution is shown in Figure 3-21. The two peaks are due to the atomic fluorine $^2P_{3/2}$ and $^2P_{1/2}$ states and the low resolution is due to the broad excimer laser linewidth. The important point is the high S/N, which exceeds 10^2 for the data presented in the figure and can be improved to $\geq 10^3$. This ensures that experiments with tagged complexes will yield adequate S/N for a number of systems, e.g., Rg–HX, CO_2–HX, N_2O–HX, HX–HY, etc.

It is our conclusion, based on the considerations and preliminary results given above, that the way is clear for size and state selection of weakly bound complexes using infrared photoexcitation. Ultrashort pulse excitation can then provide dynamics on the ground state and reach the PES at different points.

ACKNOWLEDGMENT: This article is dedicated to the memory of Richard B. Bernstein, who would have been a coauthor were he with us. The consummate perfectionist, he saw achievement as vehicular to greater progress. His tireless enthusiasm was infectious. Dick Bernstein was an optimist.

REFERENCES

Alagia, M.; Balucani, N.; Casavecchia, P.; Stranges, D.; Volpi, G. G. 1993 J. Chem. Phys. 98:8341

Alimi, R.; Gerber, R. B. 1990 Phys. Rev. Lett. 64:1453

Alrichs, R.; Brode, S.; Buck, U.; DeKieviet, M.; Lauenstein, C.; Rudolph, A.; Schmidt, B. 1990 Z. Phys. D 15:341

Altman, R. S.; Marshall, M. S.; Klemperer, W. 1982 J. Chem. Phys. 77:4344

Ashfold, M. N. R.; Lambert, I. R.; Mordaunt, D. H.; Morley, G. P.; Western, C. 1992 J. Phys. Chem. 96:2938

Baiocchi, F. A.; Dixon, T. A.; Joyner, C. H.; Klemperer, W. 1981 J. Chem. Phys. 74:6544

Baiocchi, F. A.; Dixon, T. A.; Klemperer, W. 1982 J. Chem. Phys. 77:1632

Baulch, D. L.; Cox, R. A.; Hampson, R. A., Jr.; Kerr, J. A.; Troe, J.; Watson, R. T. 1984 J. Phys. Chem. Ref. Data 13:1359

Beck, D.; Engelke, F.; Loesch, H. J. 1968 Ber. Bunsenges. Phys. Chem. 72:1105

Bemish, R. J.; Wu, M.; Miller, R. E. 1994 Faraday Discuss. Chem. Soc. 97:57

Beu.; Buck, U.; Hobein, M. 1994 J. Chem. Phys. in press

Bieler, C. R.; Janda, K. C. 1990 In *Atomic and Molecular Clusters*, E. R. Bernstein, ed., Elsevier, p. 455

Bieler, C. R.; Spence, K. E.; Janda, K. C. 1991 J. Phys. Chem. 95:5058

Blais, N. B.; Cross, J. B. 1970 J. Chem. Phys. 52:3580

Block, P. A.; Bohac, E. J.; Miller, R. E. 1992 Phys. Rev. Lett. 68:1303

Bohac, E. J.; Marshall, M. D.; Miller, R. E. 1986 J. Chem. Phys. 85:4890

Bohac, E. J.; Marshall, M. D.; Miller, R. E. 1992a J. Chem. Phys. 96:6681

Bohac, E. J.; Marshall, M. D.; Miller, R. E. 1992b J. Chem. Phys. 97:4901

Bohac, E. J.; Miller, R. E. 1993a J. Chem. Phys. 98:2604

Bohac, E. J.; Miller, R. E. 1993b Phys. Rev. Lett. 71:54

Böhmer, E.; Shin, S. K.; Chen, Y.; Wittig, C. 1992 J. Chem. Phys. 97:2536

Boivineau, M.; Calve, J. L.; Castex, M. C.; Jouvet, C. 1986a Chem. Phys. Lett. 128:528

Boivineau, M.; Calve, J. L.; Castex, M. C.; Jouvet, C. 1986b Chem. Phys. Lett. 130:208

Breckenridge, W. H. 1989 Acc. Chem. Res. 22:21

Breckenridge, W. H.; Duval, M. C.; Jouvet, C.; Soep, B. 1985 Chem. Phys. Lett. 122:181

Breckenridge, W. H.; Duval, M. C.; Jouvet, C.; Soep, B. 1987 In *Structure and Dynamics of Weakly Bound Molecular Complexes*, A. Weber, ed., D. Reidel,

Amsterdam, p. 213

Breckenridge, W. H.; Jouvet, C.; Soep, B. 1986 J. Chem. Phys. 84:1443

Brouwer, L.; Cobos, C. J.; Troe, J.; DiAbal, H. R.; Crim, F. F. 1987 J. Chem. Phys. 86:6171

Brucker, G. A.; Ionov, S. I.; Chen, Y.; Wittig, C. 1992 Chem. Phys. Lett. 194:301

Brunning, J.; Derbyshire, D. W.; Smith, I. W. M.; Williams, M. D. 1988 J. Chem. Soc. Faraday Trans. 2 484:105
Buck, U. 1992 Ber. Bunsenges. Phys. Chem. 96:1275
Buck, U. 1994 J. Phys. Chem. 98:5190
Buck, U.; Ettischer, I. 1994 Faraday Discuss. Chem. Soc. 97:215
Buck, U.; Gu, X. J.; Hobein, M.; Lauenstein, C. 1988a Chem. Phys. Lett. 163:453
Buck, U.; Gu, X. J.; Hobein, M.; Lauenstein, C. 1990a Chem. Phys. Lett. 174:247
Buck, U.; Gu, X. J.; Hobein, M.; Lauenstein, C.; Rudolph, A. 1990b J. Chem. Soc. Faraday Trans. 2 286:1923
Buck, U.; Gu, X. J.; Lauenstein, C.; Rudolph, A. 1988b J. Phys. Chem. 92:5561
Buck, U.; Gu, X. J.; Lauenstein, C.; Rudolph, A. 1990c J. Chem. Phys. 92:6017
Buck, U.; Hobein, M. 1993 Z. Phys. D 28:331
Buck, U.; Hobein, M.; Schmidt, B. 1993 J. Chem. Phys. 98:9425
Buck, U.; Huisken, F.; Lauenstein, C.; Meyer, R.; Sroka, R. 1987 J. Chem. Phys. 87:6276
Buck, U.; Lauenstein, C.; Rudolph, A.; Heijmen, B.; Stolte, S.; Reuss, J. 1988c Chem. Phys. Lett. 144:396
Buck, U.; Meyer, H.; Pauly, H. 1985 In *Unsteady Fluid Motions*, Springer Lecture Notes in Physics, F. Obermeier and G. E. A. Meier, eds., Springer
Butler, L. J.; Tichich, T. M.; Likar, M. D.; Crim, F. F. 1986 J. Chem. Phys. 85:2331
Carter, C. F.; Levy, M. R.; Woodall, K. B.; Grice, R. 1973 Faraday Discuss. Chem. Soc. 55:381
Chatfield, D. C.; Friedman, R. S.; Lynch, G. C.; Truhlar, D. G. 1992a J. Phys. Chem. 96:57
Chatfield, D. C.; Friedman, R. S.; Lynch, G. C.; Truhlar, D. G. 1993 J. Chem. Phys. 98:342
Chatfield, D. C.; Friedman, R. S.; Schwenke, D. W.; Truhlar, D. G. 1992b J. Phys. Chem. 96:2414
Chatfield, D. C.; Friedman, R. S.; Truhlar, D. G. 1991a Faraday Discuss. Chem. Soc. 91:289
Chatfield, D. C.; Friedman, R. S.; Truhlar, D. G.; Garrett, B. C.; Schwenke, D. W. 1991b J. Amer. Chem. Soc. 113:486
Chen, Y.; Hoffmann, G.; Oh, D.; Wittig, C. 1989 Chem. Phys. Lett. 159:426
Chen, Y.; Hoffmann, G.; Shin, S. K.; Oh, D.; Sharpe, S.; Zeng, Y. P.; Beaudet, R. A.; Wittig, C. 1992 In *Advances in Molecular Vibrations and Collision Dynamics*, Vol. 1, J. Bowman, ed., JAI Press, Greenwich, p. 187
Clary, D. C.; Schatz, G. C. 1993 J. Chem. Phys. 99:4578
Crim, F. F. 1984 Annu. Rev. Phys. Chem. 35:657
Cross, J. B.; Blais, N. B. 1969 J. Chem. Phys. 50:4108
Cross, J. B.; Blais, N. B. 1971 J. Chem. Phys. 55:3970
Davis, D. D.; Fischer, S.; Schiff, R. 1974 J. Chem. Phys. 61:2213
Dayton, D. C.; Jucks, K. W.; Miller, R. E. 1989 J. Chem. Phys. 90:2631
Dübal, H. R.; Crim, F. F. 1985 J. Chem. Phys. 83:3863
Duval, M. C.; Benoist D'Azy, O.; Breckenridge, W. H.; Jouvet, C. 1986 J. Chem. Phys. 85:6324
Duval, M. C.; Jouvet, C.; Soep, B. 1985 Chem. Phys. Lett. 119:317
Duval, M. C.; Soep, B.; Breckenridge, W. H. 1991 J. Phys. Chem. 95:7145
Dykstra, C. E. 1990 J. Phys. Chem. 94:6948, and references therein
Firth, N. C.; Grice, R. 1987a Mol. Phys. 60:1261
Firth, N. C.; Grice, R. 1987b Mol. Phys. 60:1273
Firth, N. C.; Keane, N. W.; Smith, D. J.; Grice, R. 1987a Faraday Discuss. Chem. Soc. 84:53
Firth, N. C.; Smith, D. J.; Grice, R. 1987b Mol. Phys. 61:859
Fisk, G. A.; McDonald, J. D.; Herschbach, D. R. 1967 Faraday Discuss. Chem. Soc. 44:228
Fleming, P. R.; Li, M.; Rizzo, T. R. 1991a J. Chem. Phys. 94:2425
Fleming, P. R.; Li, M.; Rizzo, T. R. 1991b J. Chem. Phys. 95:865
Fleming, P. R.; Luo, X.; Rizzo, T. R. 1991c In *Mode Selective Chemistry*, B. Pullman and J. Jortner, eds., Kluwer, Dordrecht
Fleming, P. R.; Rizzo, T. R. 1991 J. Chem. Phys. 95:1461
Fraser, G. T.; Pine, A. S.; Suenram, R. D.; Dayton, D. C.; Miller, R. E. 1989 J. Chem. Phys. 90:1330
Friedman, R. S.; Truhlar, D. G. 1991 Chem. Phys. Lett. 183:539
Frost, M. J.; Salh, J. S.; Smith, I. W. M. 1991a J. Chem. Soc. Faraday Trans. 2 87:1037
Frost, M. J.; Sharkey, P. ; Smith, I. W. M. 1991b Faraday Discuss. Chem. Soc. 91:305
Frost, M. J.; Sharkey, P.; Smith, I. W. M. 1993 J. Phys. Chem. 97:12254
Garcia-Vela, A.; Gerber, R. B.; Valentini, J. J. 1991 Chem. Phys. Lett. 186:223
Garcia-Vela, A.; Gerber, R. B.; Valentini, J. J. 1992 J. Chem. Phys. 97:3297
Gardiner, W. C., Jr. 1977 Acc. Chem. Res. 10:326
Girard, B.; Billy, N.; Gouédard, G.; Vigué J. 1987 Faraday Discuss. Chem. Soc. 84:65
Girard, B.; Billy, N.; Gouédard, G.; Vigué, J. 1991 Europhys. Lett. 14:13
Gordon, E. B.; Nadkhin, A. I.; Sotnichenko, S. A.; Boriev, I. A. 1982 Chem. Phys. Lett. 86:209
Green, W. H., Jr.; Moore, C. B.; Polik, W. F. 1992 Annu. Rev. Phys. Chem. 43:307
Green, W. H.; Mahoney, A. J.; Zheng, Q.-K.; Moore, C. B. 1991 J. Chem. Phys. 94:1961
Gruebele, M.; Sims, I. R.; Potter, E. D.; Zewail, A. H. 1991 J. Chem. Phys. 95:7763
Haugen, H. K.; Weitz, E.; Leone, S. R. 1985 Chem. Phys. Lett. 119:75
Hernández, M. I.; Clary, D. C. 1994 J. Chem. Phys. 101:2779
Hernandez, R.; Miller, W. H. 1993 Chem. Phys. Lett. 214:129

Hernandez, R.; Miller, W. H.; Moore, C. B.; Polik, W. F. 1993 J. Chem. Phys. 99:950
Hoffmann, G.; Ohr D.; Chen, Y.; Engel, Y. M.; Wittig, C. 1990 Israel J. Chem. 30:115
Hoffmann, G.; Oh, D.; Iams, H.; Wittig, C. 1989a Chem. Phys. Lett. 155:356
Hoffmann, G.; Oh, D.; Wittig, C. 1989b J. Chem. Soc. Faraday Trans. 2 85:1141
Hoffmann, S. M. A.; Smith, D. J.; Grice, R. 1983 Mol. Phys. 49:621
Hofmann, H.; Leone, S. R. 1978 Chem. Phys. Lett. 54:314
Hu, A; Sharpe, S. W. 1994 unpublished
Huisken, F.; Kulcke, A.; Laush, C.; Lisy, J. M. 1991 J. Chem. Phys. 95:3924
Huisken, F.; Stemmler, M. 1988 Chem. Phys. Lett. 144:391
Huisken, F.; Stemmler, M. 1992 Z. Phys. D 24:277
Hunter, M.; Reid, S. A.; Robie, D. C.; Reisler, H. 1993 J. Chem. Phys. 99:1093
Ionov, S. I.; Brucker, G. A.; Jaques, C.; Chen, Y.; Wittig, C. 1993a J. Chem. Phys. 99:3420
Ionov, S. I.; Brucker, G. A.; Jaques, C.; Valachovic, L.; Wittig, C. 1992 J. Chem. Phys. 97:9486
Ionov, S. I.; Brucker, G. A.; Jaques, C.; Valachovic, L.; Wittig, C. 1993b J. Chem. Phys. 99:6553
Ionov, S. I.; Ionov, P. I.; Wittig, C. 1994 Faraday Discuss. Chem. Soc. 97:391
Jacobs, A.; Volpp, H. R.; Wolfrum, J. 1994 Chem. Phys. Lett. 218:51
Jacobs, A.; Wahl, M.; Weller, R.; Wolfrum, J. 1989 Chem. Phys. Lett. 158:161
Jonah, C. D.; Mulac, W. A.; Zeglinski, P. 1984 J. Phys. Chem. 88:4100
Jouvet, C.; Boivineau, M.; Duval, M. C.; Soep, B. 1987 J. Phys. Chem. 91: 5416
Jouvet, C.; Duval, M. C.; Soep, B.; Breckenridae, W. H.; Whitham, C.; Visticot, J. P. 1989 J. Chem. Soc. Faraday Trans. 2 85:1133
Jouvet, C.; Soep, B. 1983 Chem. Phys. Lett. 96:426
Jouvet, C.; Soep, B. 1984 J. Chem. Phys. 80:2229
Jouvet, C.; Soep, B. 1985 Laser Chem. 5:157
Kudla, K.; Koures, A. G.; Harding, L. B.; Schatz, G. C. 1992 J. Chem. Phys. 96:7465
Kudla, K.; Schatz, G. C. 1991 J. Phys. Chem. 95:8267
Kudla, K.; Schatz, G. C.; Wagner, A. F. 1991 J. Chem. Phys. 95:1635
Lee, L. C. 1985 J. Phys. B 18:L293
Lee,Y. T.; LeBreton, P. R.; McDonald, J. D.; Herschbach, D. R. 1969 J. Chem.Phys. 51:455
Lee,Y. T.; McDonald, J. D.; LeBreton, P. R.; Herschbach, D. R. 1968 J. Chem. Phys. 49:2447
Lee, Y. T.; Valentini, J. J.; Auerbach, D. J. 1977 J. Chem. Phys. 67:4866
Legon, A. C.; Willoughby, L. C. 1985 J. Mol. Struct. 131:159
Lin, Y.; Wittig, C.; Beaudet, R. A. n.d. unpublished
Loesch, H. J.; Beck, D. 1971 Ber. Bunsenges. Phys. Chem. 75:736
Loison, J. C.; Dedonder-Lardeux, C.; Jouvet, C.; Solgadi, S. 1994 Faraday Discuss. Chem. Soc. 97:379
Lovejoy, C. M.; Schuder, M. D.; Nesbitt, D. J. 1987 J. Chem. Phys. 86:5337
Lovejoy, E. R.; Kim, S. K.; Moore, C. B. 1992 Science 256:1541
Luo, X.; Fleming, P. R.; Seckel, T. A. ; Rizzo, T. R. 1990 J. Chem. Phys. 93:9194
Luo, X.; Rizzo, T. R. 1990 J. Chem. Phys. 93:8620
Luo, X.; Rizzo, T. R. 1991 J. Chem. Phys. 94:889
Lynch, G. C.; Halvick, P.; Zhao, M.; Truhlar, D. G.; Yu, C. H.; Kouri, D. J.; Schwenke, D. W. 1991 J. Chem. Phys. 94:7150
Magnotta, F.; Nesbitt, D. J.; Leone, S. R. 1981 Chem. Phys. Lett. 83:21
Manolopoulos, D. E.; Stark, K.; Werner, H. J.; Arnold, D. W.; Bradforth, S. E.; Neumark, D. M. 1993 Science 262:1852
Manthe, U.; Miller, W. H. 1993 J. Chem. Phys. 99:3411
Marshall, P.; Fontijn, A.; Melius, C. F. 1987 J. Chem. Phys. 86:5540
Marshall, P.; Ko, T.; Fontijn, A. 1989 J. Phys. Chem. 93:1922
Miller, W. H.; Hernandez, R.; Moore, C. B.; Polik, W. F. 1990 J. Chem. Phys. 93:5657
Miyawaki, J.; Tsuchizawa, T.; Yamanouchi, K.; Tsuchiya, S. 1990 Chem. Phys. Lett. 165:168
Miyawaki, J.; Yamanouchi, K.; Tsuchiya, S. 1991 Chem. Phys. Lett. 180:287
Miyawaki, J.; Yamanouchi, K.; Tsuchiya, S. 1993 J. Chem. Phys. 99:254
Mozurkewich, M.; Lamb, J. J.; Benson, S. W. 1984a J. Phys. Chem. 88:6429
Mozurkewich, M.; Lamb, J. J.; Benson, S. W. 1984b J. Phys. Chem. 88:6435
Nesbitt, D. J. 1988 Chem. Rev. 88:843, and references therein
Nesbitt, D. J.; Lovejoy, C. M. 1990 J. Chem. Phys. 93:7716
Nesbitt, D. J.; Lovejoy, C. M. 1992 J. Chem. Phys. 96:5712
Neumark, D. M. 1992 Acc. Chem. Res. 26:33
Novick, S. E.; Janda, K. C.; Klemperer, W. 1977 J. Chem. Phys. 65:5115
Oldershaw, G. A.; Porter, D. A. 1969 Nature 223:490
Pechukas, P.; Light, J. C. 1965 J. Chem. Phys. 42:3281
Peskin, U.; Reisler, H.; Miller, W. H. 1994 J. Chem. Phys. 101:8874
Polik, W. F.; Guyer, D. R.; Miller, W. H.; Moore, C. B. 1990a J. Chem. Phys. 92:3471
Polik, W. F.; Guyer, D. R.; Moore, C. B. 1990b J. Chem. Phys. 92:3453
Polik, W. F.; Moore, C. B.; Miller, W. H. 1988 J. Chem. Phys. 89:3584
Radhakrishnan, G.; Buelow, S.; Wittig, C. 1986 J. Chem. Phys. 84:727
Randall, R. W.; Walsh, M. A.; Howard, B. J. 1988 Faraday Discuss. Chem. Soc. 85:1
Ravishankara, R. R.; Thompson, R. L. 1983 Chem. Phys. Lett. 99:377
Reid, S. A.; Brandon, J. T.; Hunter, M.; Reisler, H. 1993a J. Chem. Phys. 99:4860

Reid, S. A.; Reisler, R. 1994 J. Chem. Phys. 101:5683
Reid, S. A.; Robie, D. C.; Reisler, H. 1994 J. Chem. Phys. 100:4256
Reisler, H.; Keller, H. M.; Schinke, R. 1994 Comments At. Mol. Phys. 30:191
Rice, J. K.; Lovas, F. J.; Fraser, G. T.; Suenram, R. D. 1995 J. Chem. Phys. 103:3877
Rizzo, T. R.; Hayden, C. C.; Crim, F. F. 1983 Faraday Discuss. Chem. Soc. 75:276
Sannigrahi, A. B.; Peyerimhoff, S. D. 1986 Int. J. Quantum Chem. 30:413
Schatz, G. C. 1989 Rev. Mod. Phys. 61:669
Schatz, G. C.; Dyck, J. 1992 Chem. Phys. Lett. 188:11
Schatz, G. C.; Fitzcharles, M. S. 1988 In *Selectivity in Chemical Reactions*, J. C. Whitehead, ed., Kluwer, Dordrecht, p. 353
Schatz, G. C.; Fitzcharles, M. S.; Harding, L. B. 1987 Faraday Discuss. Chem. Soc. 84:359
Scherer, N. F.; Khundkar, L. R.; Bernstein, R. B.; Zewail, A. H. 1987 J. Chem. Phys. 87:1451
Scherer, N. F.; Sipes, C.; Bernstein, R. B.; Zewail, A. H. 1990 J. Chem. Phys. 92:5239
Schneider, L.; Meier, W.; Welge, K. H.; Ashfold, M. N. R.; Western, C. M. 1990 J. Chem. Phys. 92:7027
Segall, J.; Wen, Y.; Singer, R.; Wittig, C.; Garcia-Vela, A.; Gerber, R. B. 1993 Chem. Phys. Lett. 207:504
Segall, J.; Zhang, J.; Dulligan, M.; Beaudet, R. A.; Wittig, C. 1994 Faraday Discuss. Chem. Soc. 97:195
Sharpe, S. W.; Sheeks, R.; Wittig, C.; Beaudet, R. A. 1988 Chem. Phys. Lett. 151:267
Sharpe, S. W.; Zeng, Y. P.; Wittig, C.; Beaudet, R. A. 1990 J. Chem. Phys. 92:943
Shea, J. A.; Read, W. G.; Campbell, E. J. 1983 J. Chem. Phys. 79:614
Shin, S. K.; Chen, Y.; Böhmer, E.; Wittig, C. 1992 In *The Dye Laser*: 20 Years, M. Stuke, ed., Springer-Verlag, Berlin, p. 57
Shin, S. K.; Chen, Y.; Nickolaisen, S.; Sharpe, S. W.; Beaudet, R. A.; Wittig, C. 1991a In *Advances in Photochemistry*, Vol. 16, D. Volman, G. Hammond, and D. Neckers, eds., Wiley, New York, p. 249
Shin, S. K.; Chen, Y.; Oh, D.; Wittig, C. 1990 Philos. Trans. R. Soc. Lond. Ser. A 332:361
Shin, S. K.; Wittig, C.; Goddard, W. A., III. 1991b J. Phys. Chem. 95:8048
Sims, I. R.; Gruebele, M.; Potter, E. D.; Zewail, A. H. 1992 J. Chem. Phys. 97:4127
Sinha, A.; Vander Wal, R. L.; Crim, F. F. 1990 J. Chem. Phys. 92:401
Smith, I. W. M. 1977 Chem. Phys. Lett. 49:112
Smith, I. W. M. 1980 *Kinetics and Dynamics of Elementary Gas Reactions*, Butterworths, London, p. 202
Smith, I. W. M.; Zellner, R . 1973 J. Chem. Soc. Faraday Trans. 2 69:1617
Soep, B. 1994 unpublished
Spencer, D. J.; Wittig, C. 1979 Optics Lett. 4:1
Stockman, P. A.; Blake, G. A. 1993 Chem. Phys. Lett. 212:298
Tichich, T. M.; Likar, M. D.; Dtbal, H. R.; Butler, L. J.; Crim, F. F. 1987 J. Chem. Phys. 87:5820
Tichich, T. M.; Rizzo, T. R.; DUbal, H. R.; Crim, F. F. 1986 J. Chem. Phys. 84:1508
Trickl, T.; Wanner, J. 1983 J. Chem. Phys. 78:6091
Truhlar, D. G.; Schwenke, D. W.; Kouri, D. J. 1990 J. Phys. Chem. 94:7346
Viste, A.; Pyykkö, P. 1984 Int. J. Quantum Chem. 25:223
Walch, S. P. 1993 J. Chem. Phys. 98:1170
Walker, A. R. H.; Chen, W.; Novick, S. E.; Bean, B. D.; Marshall, N. D. submitted
Warnatz, J. 1984 In *Combustion Chemistry*, W. C. Gardiner, ed., Springer-Verlag, New York, p. 197
Wen, Y.; Segall, J.; Dulligan, M.; Wittig, C. 1994 J. Chem. Phys. 101:5665
Wiesenfeld, J. R.; Wolk, G. L. 1978a J. Chem. Phys. 69:1797
Wiesenfeld, J. R.; Wolk, G. L. 1978b J. Chem. Phys. 69:1805
Wittig, C.; Engel, Y. M.; Levine, R. D. 1988a Chem. Phys. Lett. 153:411
Wittig, C.; Ionov, S. I. 1994 J. Chem. Phys. 100:4714
Wittig, C.; Sharpe, S.; Beaudet, R. A. 1988b Acc. Chem. Res. 21:341
Wright, S. A.; Tuchler, M. F.; McDonald, J. D. 1994 Chem. Phys. Lett. 226:570
Xu, Z.; Koplitz, B.; Wittig, C. 1987 J. Chem. Phys. 87:1062
Xu, Z.; Koplitz, B.; Wittig, C. 1988 J. Phys. Chem. 92:5518
Zellner, R.; Steinert, W. 1976 Int. J. Chem. Kin. 8:397
Zeng, Y. P.; Sharpe, S. W.; Shin, S. K.; Wittig, C.; Beaudet, R. A. 1992 J. Chem. Phys. 97:5392
Zewail, A. H. 1988 Science 242:1645, and references therein
Zewail, A. H. 1993 J. Phys. Chem. 97:12427, and references therein
Zhang, J.; Dulligan, M.; Wittig, C. n.d. unpublished